AN INVESTIGATION OF HYDROGEN STORAGE IN CARBON NANOTUBES VIA COMPUTATIONAL MM METHODS

by

Güven Atay

B.S. in Ch.E., Boğaziçi University, 2002

Submitted to the Institude for Graduate Studies in
Science and Engineering in partial fulfillment of
the requirements for the degree of
Master of Science
in
Chemical Engineering

Boğaziçi University

2005

ACKNOWLEDGEMENTS

This study bears the mark of a wide array of people, whose existence provided me relief, scientific zeal and joy at times. I would like to express my sincere gratitude to my thesis supervisor, Assoc. Prof. A.Erhan Aksoylu, for his Jedi patience, guidance and help throughout my thesis. He always trusted in me and were always available with their effective contributions.

Heartfelt thanks go to Tuğba Davran and Aslıhan Sümer for the intimate friendship, support and alliance that they provided. They were ready to help me whenever I needed as well as Erdem Günay. Apart from those cited above, my appreciations are for the whole CATREL team.

I wish to thank my valuable colleagues, my “life-long partners”, Kerem Uz, İlim Çağıran, Onur Dede, Sabri and Serhat Güdemezoğlu for their friendship and relentless encouragement. My heartfelt appreciations go to my cousins, Burcu and Çiğdem for their sincere interest and computer support.

Last but not least, I would like to epress my deep gratitude to my family. Their existance has been the greatest support throughout my life. They always trusted in me even in times that, I, myself, did not and never let me give up when I lost my desire to continue. Finally, this work is dedicated to my parents, Bahattin and Ümran Atay, without whom I am sure that I could not achieve anything.

This work was supported by DPT via projects 01K120300 and 03K120250.

ABSTRACT

AN INVESTIGATION OF HYDROGEN STORAGE IN CARBON NANOTUBES VIA COMPUTATIONAL MM METHODS

In this study, hydrogen storage behaviour of single wall carbon nanotubes was investigated using moleculer mechanics. Accelerys' Discover Minimization module was employed with COMPASS (Condensed-phase Optimized Molecular Potentials for Atomistic Simulation Studies) forcefield. For the simulations, single wall CNT bundles, which have supercells of four nanotubes in triangular array with 8 layers long, were built in the computer via using the code VISUALIZER. In order to study the relation between nanotube size and hydrogen storage capacity, armchair nanotubes which have three different sizes, (5,5), (6,6) and (7,7), were used in the supercells. Simulations were carried out firstly by varying the number of hydrogen molecules only inside the nanotubes and then with different combinations of the amounts of hydrogen molecules inside nanotubes together with the hydrogen molecules at interstitial spaces between nanotubes in the bundles. In all simulations, the hydrogen storage capacity that gives minimum total energy for the system, i.e. nanotube bundle and the stored hydrogen molecules, was searched. In the simulations, chemisorption of hydrogen on nanotube walls was not considered; only physisorption of hydrogen as free hydrogen molecules in nanotubes was counted. Simulation results of the systems were examined for searching the favorable hydrogen storage according to change in the total energy of the system. Favorable hydrogen storage only inside of nanotubes for (5,5), (6,6) and (7,7) CNTs are about 2.44, 5.00, 8.20 wt. per cent, respectively. On the other hand, storage of hydrogen molecules at the interstitial spaces was found not favorable based on the total energy of the system. Stored hydrogen in all nanotubes showed a general trend; due to both the narrow diameter of nanotubes and strong van der Waals forces led by short distance between molecules, hydrogen molecules inside nanotubes condense to a molecular shell having the tube shape. It is concluded that (i) the repulsive forces determine the hydrogen storage capacity inside nanotubes and the

stability of the nanotubes; (ii) hydrogen storage data showed that hydrogen storage is linearly dependent to radius of the nanotubes as expected. Considering the fact that the volume and the number of hydrogen molecules increases with a square of the radius, whereas the number of carbon atoms increases linearly with the radius, the latter was an expected result.

ÖZET

KARBON NANOTÜPLERDE HİDROJEN DEPOLANMASININ MOLEKÜLER MEKANİK METOTLAR İLE İNCELENMESİ

Bu çalışmada, tek duvarlı karbon nanotüplerin hidrojen depolama tutumu araştırılmıştır. Simulasyon hesaplamaları için Accelerys'in "Discover Minimization" modülü COMPASS güçalanı ile birlikte kullanılmıştır. Simulasyonlar için üçgen dizilişli sekiz katmanlı dört nanotüp içeren süperhücrelerden oluşan karbon nanotüp demetleri "VISUALIZER" modülü kullanılarak oluşturuldu. Nanotüp boyutu ile hidrojen depolama kapasitesi arasındaki bağıntıyı araştırmak için üç boyutta nanotüp, (5,5), (6,6) ve (7,7), süperhücrelerde kullanılmıştır. Simulasyonlar ilk olarak sadece nanotüplerin içindeki hidrojen molekülü miktarını değiştirerek, daha sonra nanotüplerin içindeki hidrojen miktarı ile demetteki nanotüplerin arasındaki hidrojen miktarının değişik kombinasyonları denenerek yürütülmüştür. Bütün simulasyonlarda, nanotüp demeti ve depolanmış hidrojenlerden oluşan sistem için en az enerjiyi sağlayan hidrojen depolama kapasitesi aranmıştır.Simulasyonlarda hidrojenlerin nanotüp duvarlarına kimyasal olarak bağlanması dikkate alınmadı, sadece serbest hidrojen olarak depolanması göz önüne alınmıştır. Simulasyon sonuçları, sistemin toplam enerjisindeki değişime göre en elverişli hidrojen depolama kapasitesini aramak için incelendi. (5,5), (6,6) ve (7,7) nanotüplerin sadece nanotüp içindeki en elverişli hidrojen depolama miktarları sırasıyla ağırlık yüzdesi olarak 2.44, 5.00 ve 8.20 değerlerinde saptanmıştır. Diğer taraftan, hidrojen moleküllerinin nanotüpler arasındaki boşluklarda depolanmasının, sistemin toplam enerjisi göz önüne alındığında elverişli olmadığı saptanmıştır. Nanotüplerde depolanmış hidrojen molekülleri genel bir eğilim göstermektedir; nanotüplerin dar çapları ve güçlü van der Waals kuvvetleri nedeniyle nanotüplerin içindeki hidrojen molekülleri silindirik bir tüp şeklinde yoğunlaşmıştır. Buradan şu sonuçlar çıkarılmıştır; (i) moleküller arasındaki itici kuvvetler nanotüplerin içlerinde hidrojen depolama kapasitesini ve nanotüplerin kararlılığını belirlemektedir, (ii)hidrojen depolama verilerinin gösterdiğine göre hidrojen kapasitesi nanotüpün yarıçapı ile doğru orantılıdır. Nanotüpün iç hacmi ve hidrojen molekülleri

sayısının yarıçapın karesi ile orantılı olarak arttığı ve carbon atomlarının sayısının da yarı çap ile doğrusal olarak arttığı düşünülürse son sonuç beklenen bir saptamadır.

TABLE OF CONTENTS

LIST OF FIGURES

LIST OF TABLES

1. INTRODUCTION

The continuous increase in the level of hazardous emissions and the issue of more stringent environmental regulations have lead to the development of more efficient and less hazardous methods of power generation. Fuel cells, offering zero hazardous emission when pure hydrogen is used as the fuel, having long life with less maintenance, and creating less noise emission, seem to be one of the most promising power generation technologies for the future.

The overwhelming advantage of hydrogen as an energy source lies in the fact that in addition to being one of the most abundant found in nature, it can easily be regenerated, therefore constituting a true renewable energy source. Unfortunately, owing to the lack of a suitable storage system and a combination of both volume and weight limitations, the use of this technology has been restricted in mobile applications [1].

An economically viable hydrogen storage medium is an essential component for the hydrogen fueled systems and there is an ongoing research for advanced hydrogen storage materials [2]. Carbon nanotubes reveal diverse physical properties depending on the diameter and chirality. Several potential applications have been demonstrated so far. Large empty space, particularly inside the single-walled carbon nanotubes, provides a possibility to be applied for hydrogen storage vehicle with large storage capacity. It is always desirable to develop a new storage material with high capacity, light mass and high stability, which may be applicable for portable electronics and moving vehicles. Carbon nanotubes seem to be an ultimate alternative for this, since nanotubes are chemically stable and have low mass density. Yet hydrogen storage capacity in nanotubes is still far from being clearly understood [3].

Two main modes of hydrogen storage in carbon nanotubes have been proposed: physisorption making use of nonbonding interactions between the hydrogen and carbon atoms and chemisorption taking place by hydrogenation of the nanotube carbon atoms. Besides the experimental studies of hydrogen storage in carbon nanotubes, model calculations of chemisorption and physisorption by the nanotubes were also carried out

simultaneously. The chemisorption (that could be realized electrochemically) were studied by Density Functional Theory based methods while the physisorption were analyzed mainly by dynamic simulations in which only nonbonding interactions described by the Lennard-Jones potential are included in the potential functions used. In most recent works, the authors usually treat hydrogen molecules as spherical particles [4].

In this study, hydrogen storage in carbon nanotubes by physisorption was investigated by molecular mechanics methods.

First, types and structure of single wall carbon nanotube system to be studied was determined through literature survey. Carbon nanotube bundles of (5,5), (6,6) and (7,7) armchair carbon nanotubes were decided as structures to be examined for their hydrogen storage properties.

In the second stage, firstly the carbon nanotube bundles were formed as the supercells having four nanotubes via utilizing VISUALIZER code. Then, the total energy of the systems as well as its change were studied via utilizing molecular mechanics codes by changing the total number of stored hydrogen in order to find the total hydrogen stored inside the nanotubes which gives the minimum total energy for the system. Then, lastly, the total minimum energy was searched in similar fashion for different combinations of the amount of hydrogen stored inside the nanotubes and, at the same time, in the interstitial volume of the bundle for seeking the overall optimal storage capacity.

Finally, hydrogen storage of (5,5), (6,6) and (7,7) nanotubes were compared to find a relationship of hydrogen storage among different size of carbon nanotubes.

Chapter 2 contains background information on the importance of hydrogen energy, fuel cell, hydrogen utilization on fuel cells and available hydrogen storage methods and ends with experimental and theoretical approaches of hydrogen storage on carbon nanotubes. Chapter 3 involves the details of calculations carried out in this study, while the next section, Chapter 4, includes the methodology of this work and results obtained. Finally, major conclusions obtained and the recommendations brought for future work are presented at the end.

2. THEORY

2.1. Importance of Hydrogen Energy

The ever-growing demand for energy and the increase in environmental pollution concerns are exerting pressure for the development of cleaner fuels and more efficient processes. The conventional internal combustion process produces an array of pollutants including particulate materials, nitrogen oxides, sulfur oxides, hydrocarbons, carbon monoxide, as well as large amounts of carbon dioxide [1].

Investigations of alternative energy strategies have recently become important, particularly for future world stability. The most important property of alternative energy sources is their environmental compatibility. In line with this characteristic, hydrogen will likely become one of the most attractive energy carriers in the near future. Much research, including experimental and theoretical studies, have recently been carried out on hydrogen energy. However, it is necessary to understand the broader aspects of hydrogen energy [5].

The widespread use of hydrogen as an energy-storage medium, the so-called 'hydrogen economy', would offer the following advantages:

- Hydrogen is a non-toxic, clean energy carrier that has a high specific energy on a mass basis (e.g., the energy content of 9.5 kg of hydrogen is equivalent to that of 25 kg of gasoline [6]).
- Many production processes for hydrogen exist [7], including processes where some of the hydrogen is contributed by fossil fuels (e.g., steam reforming of natural gas or other light hydrocarbons, gasification of coal and other heavy hydrocarbons), electrolysis of water, direct and indirect thermo chemical decomposition, and processes driven directly by sunlight.
- Hydrogen may be transmitted over long distances in pipelines that to some degree provide a storage component
- Hydrogen can be used advantageously as a chemical feedstock in the petrochemical, food, microelectronics, ferrous and non-ferrous metal, chemical and polymer

synthesis, and metallurgical process industries, and as an energy carrier in clean sustainable energy systems.

- When combusted, hydrogen produces non-toxic exhaust emissions, except at some equivalence ratios (where its high flame temperature can result in significant NO_x levels in the exhaust products) [8].
- Hydrogen is a sustainable form of energy in that it can be produced from many primary sources, e.g., fossil fuels, renewables, and nuclear power; this flexibility reduces the chances of creating a hydrogen cartel similar to that set up by the Organization of Petroleum Exporting Countries (OPEC) [9].
- Compared to electricity, hydrogen can be stored over relatively long periods of time.
- Hydrogen can be utilized in all parts of the economy (e.g., as an automobile fuel and to generate electricity via fuel cells).

And following disadvantages:

- When mixed with air, hydrogen can burn in lower concentrations and this can cause safety concerns.
- Storage of hydrogen in liquid form is difficult, as very low temperatures are required to liquefy hydrogen.

2.2. Fuel Cell

The realization of a hydrogen economy is linked irrevocably with that of the fuel cell. Fuel cells are electrochemical devices that convert the chemical energy of a reaction directly into electrical energy. The basic physical structure, or building block, of a fuel cell consists of an electrolyte layer in contact with a porous anode and cathode on either side. A schematic representation of a fuel cell with the reactant/product gases and the ion conduction flow directions through the cell is shown in Figure 2.1.

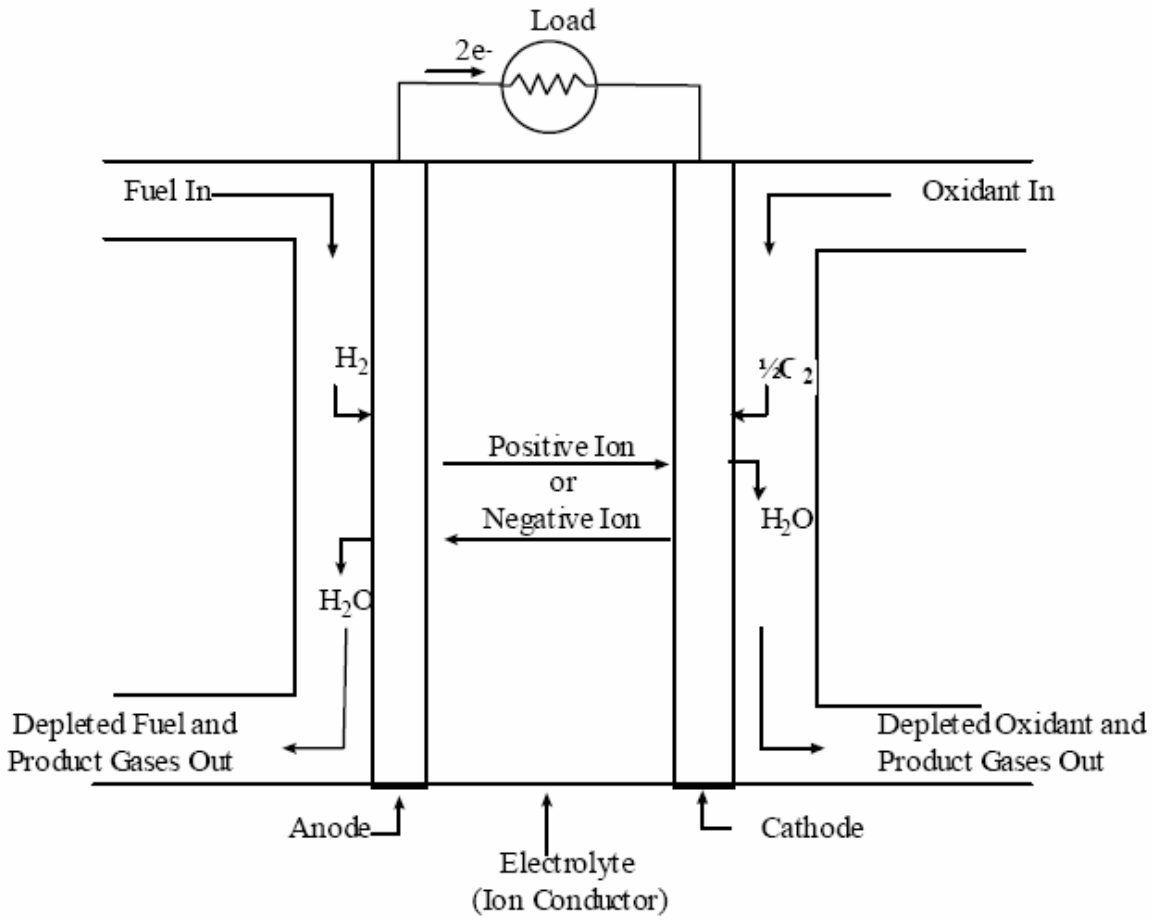

Figure 2.1 Schematic of an individual fuel cell

In a typical fuel cell, gaseous fuels are fed continuously to the anode (negative electrode) and an oxidant (i.e., oxygen from air) is fed continuously to the cathode (positive electrode); the electrochemical reactions take place at the electrodes to produce an electric current. A fuel cell, although having components and characteristics similar to those of a typical battery, differs in several respects. The battery is an energy storage device. The maximum energy available is determined by the amount of chemical reactant stored within the battery itself. The battery will cease to produce electrical energy when the chemical reactants are consumed (i.e., discharged). In a secondary battery, the reactants are regenerated by recharging, which involves putting energy into the battery from an external source. The fuel cell, on the other hand, is an energy conversion device that theoretically has the capability of producing electrical energy for as long as fuel and oxidant are supplied to the electrodes [10].

2.2.1. Fuel Cell Types

A variety of fuel cells are in different stages of development. They can be classified by use of diverse categories, depending on the combination of type of fuel and oxidant, whether the fuel is processed outside (external reforming) or inside (internal reforming) the fuel cell, the type of electrolyte, the temperature of operation, whether the reactants are fed to the cell by internal or external manifolds, etc. The most common classification of fuel cells is by the type of electrolyte used in the cells and includes:

- Polymer electrolyte fuel cell (PEFC),
- Alkaline fuel cell (AFC),
- Phosphoric acid fuel cell (PAFC),
- Molten carbonate fuel cell (MCFC),
- Solid oxide fuel cell (SOFC).

These fuel cells are listed in the order of approximate operating temperature, ranging from ~80°C for PEFC, ~100°C for AFC, ~200°C for PAFC, ~650°C for MCFC, ~600-1000°C for SOFC. The operating temperature and useful life of a fuel cell dictate the physicochemical and thermo-mechanical properties of materials used in the cell components. Aqueous electrolytes are limited to temperatures of about 200°C or lower because of their high water vapor pressure and rapid degradation at higher temperatures. The operating temperature also plays an important role in dictating the type of fuel that can be used in a fuel cell. The low-temperature fuel cells with aqueous electrolytes are, in most practical applications, restricted to hydrogen as a fuel. In high temperature fuel cells, CO and even CH_4 can be used because of the inherently rapid electrode kinetics and the lesser need for high catalytic activity at high temperature.

In low-temperature fuel cells (PEFC, AFC, PAFC), protons or hydroxyl ions are the major charge carriers in the electrolyte, whereas in the high-temperature fuel cells (MCFC and SOFC) carbonate ions and oxygen ions are the charge carriers, respectively. Major differences between the various cells are shown in Table 2.1.

Table 2.1 Summary of major differences of the fuel types

	PEFC	**AFC**	**PAFC**	**MCFC**	**SOFC**
Electrolyte	Ion Exchange Membranes	Mobilized or Immobilized Potassium Hydroxide	Immobilized Liquid Phosphoric Acid	Immobilized Liquid Molten Carbonate	Ceramic
Operating Temperature	80°C	65°C - 220°C	205°C	650°	600-1000°C
Charge Carrier	H^+	OH^-	H^+	$CO3^=$	$O^=$
External Reformer for CH_4 (below)	Yes	Yes	Yes	No	No
Prime Cell Components	Carbon-based	Carbon-based	Graphite-based	Stainless-based	Ceramic
Catalyst	Platinum	Platinum	Platinum	Nickel	Perovskites
Product Water Management	Evaporative	Evaporative	Evaporative	Gaseous Product	Gaseous Product
Product Heat Management	Process Gas + Independent Cooling Medium	Process Gas + Electrolyte Circulation	Process Gas + Independent Cooling Medium	Internal Reforming + Process Gas	Internal Reforming + Process Gas

2.2.2. Characteristics

Fuel cells have many characteristics that make them favorable as energy conversion devices. Efficiencies of present fuel cell plants are in the range of 40 to 55 per cent based on the lower heating value (LHV) of the fuel. Hybrid fuel cell/reheat gas turbine cycles that offer efficiencies greater than 70 per cent LHV, using demonstrated cell performance, have been proposed. In addition, fuel cells operate at a constant temperature, and the heat from the electrochemical reaction is available for cogeneration applications. Because fuel cells operate at nearly constant efficiency, independent of size, small fuel cell plants operate nearly as efficiently as large ones. Thus, fuel cell power plants can be configured in a wide range of electrical output, ranging from watts to megawatts. Fuel cells are quiet and, even though fuel flexible, they are sensitive to certain fuel contaminants that must be minimized in the fuel gas. The two major impediments to the widespread use of fuel cells are 1) high initial cost and 2) high-temperature cell endurance. These two aspects are the major focus of manufacturers' technological efforts.

Other characteristics that fuel cells and fuel cell plants offer are

- Direct energy conversion (no combustion).
- No moving parts in the energy converter.
- Quiet.
- Demonstrated high availability of lower temperature units.
- Siting ability.
- Fuel flexibility.
- Demonstrated endurance/reliability of lower temperature units.
- Good performance at off-design load operation.
- Modular installations to match load and increase reliability.
- Remote/unattended operation.
- Size flexibility.
- Rapid load following capability.

General negative features of fuel cells include

- Market entry cost high; N_{th} cost goals not demonstrated.
- Unfamiliar technology to the power industry.
- No infrastructure.

2.2.3. Advantages and Disadvantages

The fuel cell types have significantly different operating regimes. As a result, their materials of construction, fabrication techniques, and system requirements differ. These distinctions result in individual advantages and disadvantages that govern the potential of the various cells to be used for different applications.

PEFC: The PEFC has a solid electrolyte. As a result, this cell exhibits excellent resistance to gas crossover. The cell operates at a low 80°C. This results in a capability to bring the cell to its operating temperature quickly, but the rejected heat cannot be used for cogeneration or additional power. Test results have shown that the cell can operate at very

high current densities compared to the other cells. However, heat and water management issues may limit the operating power density of a practical system. The PEFC tolerance for CO is in the low ppm level for low temperature PEFC but can be in many thousands of ppm for emerging high temperature PEFC designs.

AFC: The AFC was one of the first modern fuel cells to be developed, beginning in 1960. The application at that time was to provide on-board electric power for the Apollo space vehicle. Desirable attributes of the AFC include its excellent performance on H_2 and O_2 compared to other candidate fuel cells due to its active O_2 electrode kinetics and its flexibility to use a wide range of electro catalysts, an attribute that provides development flexibility. Developers recognized that pure H_2 would be required in the fuel stream, because CO_2 in any reformed fuel reacts with the KOH electrolyte to form a carbonate, reducing the electrolyte's ion mobility. At the time, investigations determined that scrubbing of the small amount of CO_2 within the air, coupled with purification of the hydrogen, was not cost effective and that terrestrial application of the AFC could be limited to special applications, such as closed environments, at best.

PAFC: The CO_2 in the reformed fuel gas stream and the air does not react with the electrolyte in a phosphoric acid fuel cell, but is a diluent. This attribute and the relatively low temperature of the PAFC made it a prime, early candidate for terrestrial application. Although its cell performance is somewhat lower than the alkaline cell because of the cathode's slow oxygen reaction rate, and although the cell still requires hydrocarbon fuels to be reformed into a H_2-rich gas, the PAFC system efficiency improved because of its higher temperature environment and less complex fuel conversion (no membrane and attendant pressure drop). The need for scrubbing CO_2 from the process air is also eliminated. The rejected heat from the cell is hot enough in temperature to heat water or air in a system operating at atmospheric pressure. PAFC systems achieve about 37 to 42 per cent electrical efficiency (based on the LHV of natural gas). This is at the low end of the efficiency goal for fuel cell power plants. PAFCs use high cost precious metal catalysts such as platinum. The fuel has to be reformed external to the cell, and CO has to be shifted by a water gas shift reaction to below 3 to 5 volume per cent at the inlet to the fuel cell anode or it will affect the catalyst. These limitations have prompted development of the alternate, higher temperature cells, MCFC and SOFC.

MCFC: Many of the disadvantages of the lower temperature as well as higher temperature cells can be alleviated with the higher operating temperature MCFC (approximately 650°C). This temperature level results in several benefits: the cell can be made of commonly available sheet metals that can be stamped for less costly fabrication, the cell reactions occur with nickel catalysts rather than with expensive precious metal catalysts, reforming can take place within the cell provided a reforming catalyst is added (results in a large efficiency gain), CO is a directly usable fuel, and the rejected heat is of sufficiently high temperature to drive a gas turbine and/or produce a high pressure steam for use in a steam turbine or for cogeneration. Another advantage of the MCFC is that it operates efficiently with CO_2-containing fuels such as bio-fuel derived gases. This benefit is derived from the cathode performance enhancement resulting from CO_2 enrichment.

The MCFC has some disadvantages, however: the electrolyte is very corrosive and mobile, and a source of CO_2 is required at the cathode to form the carbonate ion. Sulfur tolerance is controlled by the reforming catalyst and is low, which is the same for the reforming catalyst in all cells. Operation requires use of stainless steel as the cell hardware material. The higher temperatures promote material problems, particularly mechanical stability that impacts life.

SOFC: The SOFC is the fuel cell with the longest continuous development period, starting in the late 1950s, several years before the AFC. Because the electrolyte is solid, the cell can be cast into flexible shapes. The solid ceramic construction of the cell also alleviates any cell hardware corrosion problems characterized by the liquid electrolyte cells and has the advantage of being impervious to gas cross-over from one electrode to the other. The absence of liquid also eliminates the problem of electrolyte movement or flooding in the electrodes. The kinetics of the cell are fast, and CO is a directly useable fuel. There is no requirement for CO_2 at the cathode as with the MCFC. At the temperature of presently operating SOFCs (~1000°C), fuel can be reformed within the cell. The temperature of an SOFC is significantly higher than that of the MCFC. However, some of the rejected heat from an SOFC is needed for preheating the incoming process air.

The high temperature of the SOFC has its drawbacks. There are thermal expansion mismatches among materials, and sealing between cells is difficult in the flat plate

configurations. The high operating temperature places severe constraints on materials selection, and results in difficult fabrication processes. The SOFC also exhibits a high electrical resistivity in the electrolyte, which results in a lower cell performance than the MCFC by approximately 100 mV. Researchers would like to develop cells at a reduced temperature of 650°C, but the electrical resistivity of the presently-used solid electrolyte material would increase.

2.3. Hydrogen Utilization

2.3.1. Stationary Power

The phosphoric acid fuel cell (PAFC) is the most advanced for moderately large stationary power units. The concentrated phosphoric acid electrolyte allows the cell to operate well above the boiling point of water, which is a limitation on other acid electrolytes that require water for conductivity. Moreover, the high-operating temperature of around 200 °C enables the platinum electro catalyst to tolerate up to 1 wt.% (100 ppm) of carbon monoxide and this broadens the choice of fuel. On the other hand, the use of phosphoric acid requires the other components to resist corrosion. Turn-key systems are available commercially and over 250 PAFCs, each rated at 200kW, have been installed at locations in Asia (principally Japan), Europe, and the USA. These systems supply combined heat and power to major building complexes, such as airport terminals, hospitals, hotels, military facilities, office buildings, and schools.

Proton-exchange membrane fuel cells (PEMFCs) are also being produced in a variety of sizes for stationary power applications. The technology is very responsive to changes in electrical load and the start-time is appreciably faster than that of PAFCs (<0.1 h versus 1–4 h). In common with other types of fuel cell, single PEM cells can be stacked together, in series electrically, to form a module with a higher voltage. Field trials have been conducted on 250-kW PEMFC plants to evaluate their suitability and performance as distributed power generators for commercial and residential consumers.

There are two high-temperature fuel cells, namely, the molten carbonate fuel cell (MCFC) and the solid oxide fuel cell (SOFC). The latter is an all-solid-state device with no

liquid components. Both present difficult materials science and technology problems. Molten alkali carbonate at 600–700 ºC is a most aggressive medium and corrosion problems are severe in this fuel cell. The SOFC operates at even higher temperatures, but at least has no liquid components to cause corrosion.

The high-temperature operation of the MCFC and the SOFC systems does, however, offer some advantages, namely: (i) removes the need for a precious-metal electrocatalyst, which reduces cost; (ii) allows the reforming of fuels internally, which enables the use of a variety of fuels, simplifies the engineering (especially heat balancing), and reduces the capital cost; (iii) provides high tolerance to carbon monoxide poisoning. Despite the technical problems they pose, considerable research progress has been made, and prototypes of both MCFC (300 kW–3MW) and SOFC (100–250 kW) plants have been built and tested in several countries. Given their long start-up times (1–5 and 5–10 h, respectively) and the slow response to changing power demands, the two technologies are seen as base-load generators and as candidates for combined heat and power ('co-generation') systems. The high-operating temperatures result in exhaust heat of good quality that may be used to drive steam or gas turbines.

2.3.2. Portable Power

Rechargeable batteries are well-suited to portable power applications where the energy requirement between recharges is relatively small. In recent years, for example, lithium-ion batteries have proved their worth in mobile communications (cellular phones) and in laptop computers. With the advent of mobile broadband computing, however, the next generation of portable electronic equipment will demand ever-greater amounts of stored energy. For this reason, attention is turning to so-called 'micro fuel cells' that promise an energy-storage capability of over an order of magnitude greater than that of the best batteries. Already, there has been a surge of interest in the development of units that generate just a few watts to power a wide range of consumer electronics, as well as in larger cells. At present, the direct methanol fuel cell (DMFC) is the preferred technology because, as a liquid fuel, methanol is more readily dispensed and carried than hydrogen. Replacement of a spent methanol cartridge in a micro fuel cell will only take a few seconds. By comparison, rechargeable batteries require periods of hours to be replenished.

Furthermore, liquid methanol has a higher stored energy than hydrogen. Applications requiring higher power levels are stimulating the development of hybrid fuel cell–battery combinations, in which the battery provides the peak power when required and is recharged by the fuel cell.

2.3.3. Power for Road Transportation

Conventional internal-combustion-engined vehicles (ICEVs) are frequently designed for power rather than for economy. The result is that these vehicles have engines that are too large and inefficient for steady driving. The way to avoid this profligate waste of petroleum, and thereby, to reduce vehicle emissions is to divorce steady-state performance from acceleration by having two separate energy sources. Accordingly, many automotive companies are putting sizeable efforts into the development of hybrid electric vehicles (HEVs) that have electrical or electromechanical drive-trains.

Hybrid electric cars are of two basic types. The ‘series hybrid’ has a purely electrical transmission and drive that is powered by a rechargeable battery that is recharged by a small ICE via a generator. The engine–generator combination provides sufficient power to maintain the vehicle at a steady cruising speed. The ‘parallel hybrid’ has a conventional mechanical transmission that links the engine to the wheels. The engine is sized for cruising and is boosted when required by an electric motor. In both designs of HEV, the battery system may be augmented by the inclusion of a super capacitor, which provides an efficient means for the capture of energy from regenerative braking. To date, most hybrids have been produced with a parallel configuration. In the final analysis, the choice of hybrid system depends on the required duty cycle of the vehicle, the degree of engineering complexity, the capital and running costs, and the emission regulations that have to be observed.

The fuel-cell vehicle (FCV) operating on hydrogen, most probably with a PEMFC, is seen as the ultimate solution to the increasing energy security and environmental problems that are confronting road transportation. The appeal of FCVs to manufacturers is less obvious. At their present stage of development, PEMFC power systems are hugely more expensive than ICEs (up to 60 times greater per kW of power produced) and the ability to

reduce the costs to a competitive value must be questionable. In addition, there are numerous technical difficulties still to be resolved before FCVs can become commercially viable. Above all, there are the over-riding problems of where to manufacture the hydrogen, how to convey it to the vehicle-refuelling sites, and how to store it on board.

The efficiency of fuel cells is also a critical issue. Much is made of the fact that fuel cells are not heat engines like ICEVs, so their efficiency is not limited by the Carnot cycle, and therefore, must be high. This reasoning promotes much interest and investment in fuel-cell technology. The thermodynamic 'theoretical' efficiency, defined as the ratio of reaction free energy to enthalpy, can be above 80 per cent. In practice, the efficiency must be smaller. How much smaller is difficult to calculate and depends on numerous kinetic and other parameters, and energy consumption by the auxiliary components [4-3].

2.3.4. Barriers

Studies worldwide indicate the technical feasibility of hydrogen as an energy carrier in the transport and stationary sectors, but several non-technical barriers need to be overcome or removed before hydrogen can be deployed in energy systems.

- The primary constraint on remote fuel cells generating electricity from hydrogen is economical. For a fuel cell to compete with other generation sources, its price must be reduced dramatically. Remote power applications offer the best opportunities for fuel cells to compete economically. Generally speaking, the cost of the hydrogen should be under $10/MMBtu to be competitive with other energy sources. Fuel cells at customer sites with a use for the waste heat must be acquired and installed at a cost under $2,000/kW.
- Research and development is required to improve the performance and lower the cost of renewables, storage, and fuel cell technologies. Technologies are needed that can produce hydrogen for the same price as gasoline. Storage technologies must be developed to allow cheap, safe hydrogen storage. Finally, fuel cell technology must advance to improve efficiency.
- Safety is a prime consideration for stationary fuel cells. As fuel cells come closer to the customer, codes must be written and building inspectors educated to allow the

introduction of renewable fuel cell power systems. Standards are being developed for onboard hydrogen, but these efforts must be expanded to include standards in building codes and for on-site hydrogen production, storage, and use at industrial sites. Codes and standards activities along these lines are underway.

- Public outreach is necessary for the development of hydrogen technologies. The public perception is that hydrogen is dangerous. EPA lists hydrogen as a hazardous chemical. The public requires positive experiences in using hydrogen at work or in transportation to overcome negative perceptions. Children can be educated at school with a curriculum that includes studying hydrogen as a renewable, nonpolluting energy source.

2.4. Hydrogen Supply to a Fuel Cell

Hydrogen can either be generated on-site or be stored close to fuel cell system. These two options are briefly explained below.

2.4.1. Hydrogen Production

Of the present world-wide production of hydrogen, over 90 per cent comes from raw fossil materials [9]. Any carbonaceous material can be used to make hydrogen from steam reforming, but they are more likely to contain contaminants than natural gas, and would require cleanup before using. The main reason natural gas is used is that the supply of natural gas is abundant and the price continues to remain low. If the prices of natural gas or restrictions on the use make using natural gas impossible, water is the other abundant source [10]. Main processes for the production of hydrogen are described below.

Hydrogen from Fossil Fuels: The gasification of coal is the oldest means of obtaining hydrogen from fossil fuels.Whenheated in a restricted supply of air**,** coal is converted to mixture of hydrogen, methane and carbon monoxide **,** together with coal tar and coke. Alternatively, when heated coal is reacted with steam the ‘water-gas reaction’ occurs, i.e.,

$$C + H_2O \rightarrow CO + H_2 \tag{2.1}$$

The water-gas reaction is highly endothermic. Conversely, the combustion of coal or coke in air is highly exothermic. It is, therefore, usual to pair off the two reactions so as to balance the heat evolved with that absorbed. The resulting gas is a mixture of CO, H_2 , CO_2, and N_2. This may be upgraded in terms of hydrogen content by the 'water-gas shift reaction'. The gas is reacted with steam over a catalyst that converts carbon monoxide to carbon dioxide and increases the amount of hydrogen, i.e.,

$$CO + H_2O \rightarrow CO_2 + H_2 \tag{2.2}$$

The carbon dioxide can be removed by a variety of gas scrubbing techniques. The process engineering of coal gasification is quite complex.

The steam reforming of natural gas is the most efficient and widely used process for making hydrogen. At present, it is also the cheapest route. The methane is reacted with steam and air over a nickel-based catalyst, i.e.,

$$CH_4 + H_2O \rightarrow CO + 3H_2 \tag{2.3}$$

The resulting product is known as 'synthesis gas' (or 'syngas') because it may be used for the preparation of a range of commercial products that include hydrogen, ammonia, methanol, and various organic chemicals. As with the gasification of coal, steam reforming can be combined with the water-gas shift reaction to increase the yield of hydrogen.

A third method is 'partial oxidation' in which fuel and oxygen are combined in proportions such that the fuel is converted into a mixture of hydrogen and carbon monoxide. Depending on the composition of the fuel and the required processing rate, the partial oxidation process is carried out either catalytically or non-catalytically. The drawback to partial oxidation is that it requires the use of expensive oxygen (rather than air, which would dilute the product hydrogen with nitrogen).

Processes based on the use of fossil fuels produce carbon dioxide in addition to hydrogen appears to be self-defeating on environmental grounds. Clearly, their future will depend on developing efficient means to separate this greenhouse gas and then sequester it. Therefore, efforts are underway to develop technology that will reduce both costs and emissions.

Hydrogen can also be produced by the direct thermo-catalytic decomposition ('cracking') of methane or other hydrocarbons. The energy requirement per mole of methane is, in fact, less than for steam reforming, although only half as much hydrogen is produced, and the process is simpler. In addition, a valuable by-product clean solid carbon is produced, which obviously can be captured and stored more easily than gaseous carbon dioxide. There is, however, the problem of progressive catalyst deactivation through carbon build-up; reactivation would result in unwanted CO_2 emissions [9].

Hydrogen from Water: Water is the other huge storeroom of hydrogen. Breaking down water to hydrogen also requires energy. Electrical, chemical, light or thermal energy can be employed.

Electrolysis: Although electrolysis is a mature technology, only a few percent of world hydrogen is obtained by this method. Electrolysis is extremely energy-intensive—the faster the generation of hydrogen, the greater is the power required per kilogram produced. Consideration has also been given to operating fuel cells in reverse as electrolyzers. The dual-function system is termed a 'regenerative fuel cell'. Such technology would save on weight and costs compared with a power system that employs a separate fuel cell and electrolzyer. It would also offer the prospect of using renewable energy (e.g., solar, wind, geothermal) to generate hydrogen that would be stored in the same unit for subsequent production of electricity.

Thermo-chemical production: It is also possible to decompose water to form hydrogen without generating electricity first. This would remove the need for an electrolyzer and avoid the problem of emissions.For example, thermal energy can be used via 'thermochemical cycles'.

$$H_2SO_4 \rightarrow \frac{1}{2} O_2 + SO_2 + H_2O \quad (2.4)$$

$$SO_2 + I_2\ 2H_2O \rightarrow 2HI + H_2SO_4 + \text{heat} \quad (2.5)$$

$$2HI \rightarrow I_2 + H_2 \quad (2.6)$$

Efficiencies of around 40% have been demonstrated in the laboratory, but the processes are still far from practical realization. Thermochemical cycles are, however, obvious candidates for coupling with the waste heat from nuclear power plants.

Photoelectrolysis: Light is converted to electrical and chemical energy by using a semi-conducting oxide, such as titanium dioxide, to absorb photons and provide oxygen and electrons. The electrons flow through an external circuit to liberate hydrogen at a metal counter electrode, such as platinum. By virtue of its relatively low cost, titanium dioxide is most attractive as a photovoltaic material. It does, however, have somewhat high band-gap energy, and therefore, absorbs light energy in the ultraviolet rather than in the optical part of the spectrum. Accordingly, present efficiencies are only 1–2 per cent, well below the commercial target of 10 per cent.

Biophotolysis: Photosynthesis is the basis for almost all life on earth. The first step involves splitting water into oxygen and hydrogen, and then hydrogen is mixed with carbon dioxide and turned into carbohydrates. There are, however, some groups of micro-algae that are capable of releasing hydrogen. For example, green algae contain an enzyme, hydrogenase, it catalyzes the reduction of protons by electrons to form hydrogen. Biologically, however, the system is not designed for continuous operation. This is because the enzyme is very sensitive to oxygen and is only synthesized after several hours of dark preincubation under anaerobic conditions. To overcome this, two-stage 'indirect biophotolysis' processes are being investigated in which a photosynthetic carbon dioxide fixing stage that generates oxygen is followed by a dark anaerobic fermenting stage that produces hydrogen.

Thermolysis: The temperature required for breaking down water directly into hydrogen and oxygen can be achieved by focusing the sun rays from a large number of

individual mirrors on to a thermal receiver mounted on top of a central, tall 'solar tower'. The key scientific challenges are to find catalysts that will reduce the dissociation temperature, and to provide an improved means for separating the gases so as to prevent recombination. Much of solar radiation lies in the infra-red part of the spectrum and is of too low energy to be utilized in photoelectrochemical reactions so that it is wasted. Radiation received by the solar tower would be separated into an infra-red component to heat pressurized water and into optical/ultraviolet radiation to effect the water-splitting reaction. There is a drawback in that regions of the world where insolation is both high and persistent are often those where water is in short supply.

2.4.2. Hydrogen Storage

There are many methods for storing hydrogen; the four most common methods are:

Compressed gas in pressure vessels: New materials have allowed pressure vessels and storage tanks to be constructed that can store hydrogen at extremely high pressures.

Hydrogen absorbing materials:

- A number of metals (pure and alloyed) can combine with hydrogen to make a metal hydride. The hydride releases hydrogen when heated. Hydrogen stored in hydrides under pressure has a very high energy density.
- Hydrogen molecules that have been absorbed on charcoal can approach the storage density of liquid hydrogen.
- Small glass spheres (microspheres), carbon nanotubes, and fullerenes can hold hydrogen if it is induced at high pressures and temperatures. The hydrogen is held captive in the solid matrix when the temperature lowers. Hydrogen can be released by heating the solid.

Liquid storage: Hydrogen can be converted into a liquid by reducing the temperature to -253 ^{o}C. This can save cost in transportation, but requires additional energy and cost to keep the hydrogen at the lower temperature. Refrigerating hydrogen to liquid form uses the equivalent of 25 to 30 per cent of its energy content. A concern of storing liquid hydrogen is minimizing loss of liquid hydrogen by boil-off.

Underground storage in depleted oil and natural gas reservoirs, aquifers, and salt cavities: For underground storage of hydrogen, a large cavern of porous rock with an impermeable cap rock above it is needed to contain the gas. As much as 50 percent of the hydrogen pumped into the formation will remain in the formation.

These methods will be investigated in detail in the Section 2.5.

2.5. Hydrogen Storage

2.5.1. Gaseous and Liquid Hydrogen

Compressed hydrogen may be stored in pressure vessels. Steel cylinders are used for stationary storage at pressures of up to 80 MPa. For portable and mobile applications, however, cylinder weight and volume must obviously be minimized. There has been some success with the development of lightweight vessels composed of carbon-fiber shells with aluminum liners that can withstand a pressure of 55 MPa, and provide a hydrogen storage density of 3-4 MJ dm^{-3}, but the corresponding gravimetric targets (7.2 and 10.8 MJ kg^{-1}) will be even more difficult to reach. In this respect, liquid hydrogen would be more attractive, its density is 850 times greater than that of the gaseous form. Liquid hydrogen is routinely transported by road and by sea, but about 30% of the energy in the hydrogen is wasted in the liquefaction process, the cryogenic and filling–emptying equipment is both complex and costly, and the boil-off rate is such that the liquid can only be stored for a few days at most. Therefore, this storage option is not practical for most potential applications.

2.5.2. Metal Hydrides

Certain metals and alloys can repeatedly absorb and release hydrogen under moderate pressures and temperatures via the formation of hydrides. Heat must be removed during absorption of the hydrogen, but has to be added to effect desorption. This feature provides a safe method of storage, i.e., when the heat source is removed, the hydride ceases to expel hydrogen. The metal hydrides can be categorized as high, medium- or low-temperature systems. Clearly, hydrides operating close to ambient are preferred. Unfortunately, the maximum gravimetric storage of low-temperature hydrides is quite low,

typically 1-2 wt. percent. Moreover, the best high-temperature hydrides offer a maximum storage of only 3.6 wt. per cent (5.1 MJ kg^{-1}). Both mass and volume are critical factors when considering storage on board a vehicle. Obviously, the major research challenges are to develop new alloying techniques for low-temperature hydrides that have increased gravimetric density.

2.5.3. Chemical Storage

Hydrogen may also be stored chemically in the form of ionic salts that are composed of sodium, aluminum or boron, and hydrogen, the so-called 'complex hydrides'. The alanates $Na[AlH_4]$ and $Na_3[AlH_6]$ are the preferred reagents. Thermal decomposition of $Na[AlH_4]$ takes place in two steps, i.e.,

$$3Na[AlH_4] \rightarrow Na_3[AlH_6] + 2Al + 3H_2 \tag{2.7}$$

$$Na_3[AlH_6] \rightarrow 3NaH + Al + H_2 \tag{2.8}$$

The first step, at 50-100 ºC, corresponds to the release of 3.7 wt. per cent hydrogen and the second step, at 130-180 ºC, to a further 1.9 wt. per cent hydrogen. In the presence of a titanium catalyst, the temperatures for discharge and recharge of hydrogen may be brought down to acceptable levels.

Sodium borohydride, $NaBH_4$, is stable up to about 400 ºC, and is therefore, not suitable for providing hydrogen through a thermal-activation process. It does release hydrogen, however, on reaction with water, i.e.,

$$NaBH_4 + 2H_2O \rightarrow NaBO_2 + 4H_2 \tag{2.9}$$

This is an irreversible reaction, but has the advantage that 50% of the hydrogen comes from the water. In effect, $NaBH_4$ acts as a 'water-splitting' agent. Based on the mass of $NaBH_4$, the hydrogen released is 21 wt. per cent, but in practice this is lowered to around 7 wt.% when the total system weight is taken into account.

Organic liquids, such as cyclohexane or methanol, can serve as chemical carriers of hydrogen. The gas is subsequently recovered by catalytic decomposition. Methanol is usually manufactured from synthesis gas. Methanol derived from fossil fuel is a prime candidate for fuel cells in portable applications.

2.5.4. Carbonaceous Materials

The best performance in hydrogen storage was achieved with materials based on carbon structures of highest effective porosity. The two forms of carbon that is the most known to us are diamond and graphite. However, there are also other forms of carbon structures such as graphite nanofibers, fullerenes and nanotubes that are the newest advanced carbon structures, with special properties [11]. Although graphite nanofibers, fullerenes and nanotubes have been reported to be very promising candidates for large amount of hydrogen storage [2], activated carbons must be taken into account for hydrogen storage research.

Activated Carbons: Bulky carbon with high surface area, the so-called activated carbon, is carbon structure able to adsorb hydrogen in its microscopic pores. The main problems are that only some of the pores are small enough to catch the hydrogen atom and that high pressure must be applied in order to get the hydrogen into the pore.

About 5.2 wt. per cent of hydrogen adsorbed into the activated carbon has been achieved at cryogenic temperatures and in pressures of about 45–60 bar [12]. In ambient temperature and pressure of 60 bar, the storage capacity has been only approximately 0.5 wt. per cent [13].

David *et al*. [14] developed chemically activated carbons that absorbed about 2.2 – 2.8 wt. per cent hydrogen at cryogenic temperatures and in pressures of about 12-15 bar. For microporous carbons the details of the pores (size and shape) apparently affect the specific hydrogen uptake to a large extent. In addition to general-purpose active carbons, advanced active carbons with specific control on pore structure have been developed over the past few decades for specific applications. Research and development efforts are continuing for more and more efficient applications of these materials.

Graphite Nanofibers (GNFs): Graphite nanofibers consist of catalytically produced graphene sheets that are oriented to form various fibrous structures. The orientation of the sheets in the fibers can be controlled by the choice of catalyst. The individual graphene sheets in these structures are thought to have very small cross-sectional areas, of the order of 50 nm^2 [15]. There are contradictory data on the amount of hydrogen adsorbed by GNFs. Hydrogen adsorption of up to 60 wt. per cent at 300 K and a pressure of about 100 atm on graphite nanofibers has been reported by Rodriguez *et al*. [16], but it is not confirmed by other researchers. However, Fan *et al*. have reported 10–13 wt. per cent adsorption [17]. Computer simulation studies of hydrogen adsorption on graphitic nanofibers [18] are unable to account for the phenomenal storage capacities reported by Rodriguez *et al*., or even for the more modest values claimed by Fan *et al*.

GNFs, doped with Li and K and having cross- or cone-layer structure absorb up to 20 and 14 wt. per cent of H_2, respectively, or 160 and 112 kg H_2 per m^3. Some authors call these results into question.

Fullerenes: Fullerenes are a new class of carbon aromatic compounds with unusual structural, chemical and physical properties which, in turn, will lead to novel and unexpected applications. Fullerenes are synthesised carbon molecules usually shaped like a football, such as C_{60} and C_{70} and they are able to hydrogenate through the reaction [19]:

$$C_{60} + xH_2O + xe^- \rightarrow C_{60}H_x + xOH^- \qquad (2.10)$$

According to theoretical calculations, the most stable of these are $C_{60}H_{24}$, $C_{60}H_{36}$ and $C_{60}H_{48}$, latter of which is equal to 6.3 wt. per cent of hydrogen adsorbed [20]. An experimental study made by Chen *et al*. shows that more than 6 wt. per cent of hydrogen can be adsorbed on fullerenes at 180ºC and at about 25 bar [21]. Usually the bonds between C and H atoms are so strong that temperatures over 400ºC are needed to desorb the hydrogen [20], but Chen *et al*. were able to do this at a temperature below 225ºC [21]. Despite the quite high hydrogen-storing ability, the cyclic tests of fullerenes have shown poor properties of storing hydrogen [22].

Carbon Nanotubes (CNTs): Carbon nanotubes are explained in Section 2.6 in more detailed fashion other than carbonaceous structures.

2.6. Hydrogen Storage in Carbon Nanotubes

Nanotubes are manufacturing from pure carbon. Pure carbons only have two covalent bonds sp^2 and sp^3, the former constitutes graphite and the latter constitutes diamond. sp^2 is a strong bond within a plane but weak between planes. When more sp^2 bonds together, they form six-fold structures, like honey comb pattern, which is a plane structure, the same structure as graphite. Graphite is stacked layer by layer so it is only stable for one single sheet. Carbon nanotubes were discovered in 1991 by Iijima [23] accidentally when synthesising fullerenes [11]. CNTs are the result of the seamless rolling up of one or several graphite sheets over themselves [24]. Tubes formed by only one single graphite layer are called single wall nanotubes (SWNT). Tubes consisting of multiple concentric graphite layers are called multi-wall nanotubes (MWNT) [25]. Depending the relative orientation of the rolling axis with respect to underlying graphite structure, one can have nanotubes with different helicities. Three types of SWNTs are shown in Figure 2.2.

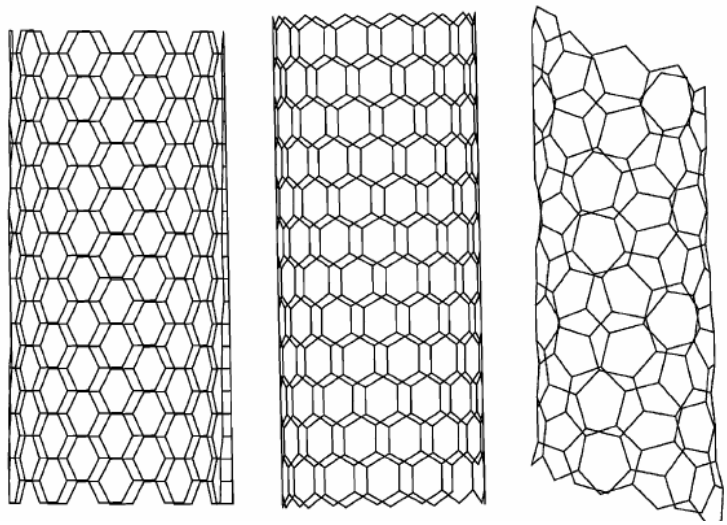

Figure 2.2 Armchair (10,10), zigzag (14,0) and chiral (7,3) nanotubes.

Nanotubes are the strongest carbon fibers that are currently known. A single-wall nanotube can be up to 100 times stronger than that of steel with the same weight while the density is only 1.3 g/cm3 . That means that materials made of nanotubes are lighter and more durable [11].

Carbon nanotubes have attracted much expectation to store hydrogen because they have cylindrical structures and hollow spaces inside of their sidewalls [26]. Two main modes of hydrogen storage in carbon nanotubes have been proposed: physisorption making use of nonbonding interactions between the hydrogen and carbon atoms and chemisorption taking place by hydrogenation of the nanotube carbon atoms [4].

2.6.1. Experimental Studies

Dillon *et al*., the first to publish reports of hydrogen adsorption by SWNTs, investigated by thermal desorption spectroscopy the hydrogen storage capacity of non-purified bundles of SWNTs [27]. Hydrogen storage capacity for pure SWNTs was estimated as 5–10 wt. per cent at pressures less than 0.1 MPa near room temperature by assuming that this hydrogen content is due to the small fraction of SWNTs present in the sample. Ye *et al*. [28] reported a storage capacity of 8 wt. per cent for purified single-walled carbon nanotubes. This high value was obtained at 80 K and for a hydrogen pressure of 12 MPa. Liu *et al*. [29] showed by volumetric measurements on SWNTs with large mean diameters of 1.85 nm a reproducible storage capacity of 4.2 wt. per cent at room temperature and 10 MPa H_2 pressure. Furthermore, most of the stored hydrogen can be released under ambient pressure were reported at room temperature. Again it should be noted, that none of these experiments could be repeated or confirmed independently in other laboratories up to now.

2.6.2. Theoretical Studies

Simultaneously to experimental studies of hydrogen storage in SWNTs, model calculations of chemisorption and physisorption by the nanotubes were carried out. The former were studied by DFT-based methods while the latter were analyzed mainly by Monte Carlo dynamic simulations in which only nonbonding interactions described by the Lennard-Jones potential are in included in the potential functions used. In the latter works the authors usually treat hydrogen molecules as spherical particles and carry out the calculations only for, mostly unspecified explicitly, armchair nanotubes [4].

Although high H_2 uptake values obtained from experimental studies, most of the theoretical and numerical studies agree, predicting a relatively low storage capacity in purified carbon nanotubes at room temperature. For example, Guay *et al*. carried out Monte Carlo simulations of hydrogen adsorption on carbon nanotubes at room temperature (293 K) and moderate pressure (10 MPa) [30]. For the zigzag type SWNT models considered, the most stable hexagonal arrangement of nanotubes within a bundle was used. The standard unit cell, where periodic boundary conditions were applied and the intratubular and intertubular adsorption sites were also identified. Their simulations indicate that pure carbon nanostructures could not reach a hydrogen uptake of 6.0 wt. per cent (or 60 kg/m^3 for volumetric densities that is target capacity for a practical hydrogen storage material for use in vehicles). For standard carbon nanotubes, the amount of adsorbed hydrogen is 0.6-1.4 wt. per cent.

Another work by Dodziuk *et al*. [4] investigated hydrogen absorption on armchair, zigzag and chiral CNTs by molecular modeling calculations. The calculations were carried out for three types of nanotubes with different amount of hydrogen molecules and for the bundle consisting of seven armchair nanotubes. The calculations showed that there is no essential difference among armchair, zigzag and chiral nanotubes as concerns their ability to host hydrogen molecules inside them. The total amount of the hydrogen inside the nanotubes is very small and H_2 molecules outside the nanotubes do not 'stick' to them at higher temperatures. This result agrees with the conclusions reached by some other groups on the basis of different models. Therefore, it seems that the literature reports on the very high hydrogen intake in carbon nanotubes cannot be obtained by physisorption process.

It is worth noting that a recent theoretical study reported that (10,10) nanotubes could hold up to 14 wt. per cent hydrogen [3]. This study is unfortunately somewhat misleading. The authors use electronic density functional theory and a tight-binding formalism to study the geometry and chemical binding properties of atomic hydrogen inside and outside of an isolated SWNT. Tight binding studies can be very useful for chemically bonded species, but they do not give any information on long-range electron correlation, which is responsible for the physisorption phenomenon. Notably, the study indicates that chemisorption of atomic hydrogen on each carbon atom inside a nanotube is energetically unstable. The system relaxes to form molecular hydrogen inside the nanotube. However,

their estimate of 14 wt. per cent is not realistic because the binding energies of the hydrogen molecules are reduced by about 2 eV per molecule, indicating that the corresponding bulk pressure would have to be extraordinarily high, probably in the GPa range.

3. CALCULATIONS

3.1. Calculation Methods

3.1.1. Density Functional Theory (DFT)

The 1998 Nobel Prize for Chemistry was awarded to Walter Kohn for his development of density functional theory. Dirac stated in 1929 that, "the fundamental laws necessary for the mathematical treatment of large parts of physics and the whole of chemistry are thus fully known, and the difficulty lies only in the fact that application of these laws leads to equations that are too complex to be solved.".

The difficulty lies in what is known as many-body theory: once more than three objects are interacting in some way (e.g. the Sun, the Moon and the Earth interacting through gravity, or three electrons through electromagnetism) the equations of motion become analytically insoluble. When considering the behavior of electrons in a solid, as is the main task of electronic structure theory, the interaction of the electrons provides the main problem. What Hohenberg and Kohn showed in 1964 was that to find the energy of a collection of electrons, the electron density was all that was necessary, not the motion of the individual electrons. Kohn and Sham then showed in 1965 that this theory could be rewritten to give a set of equations for non-interacting electrons with all of the many-body interactions in a single term (the exchange and correlation energy) which depends on the electron density. This many-body term has to be approximated to perform calculations, but a relatively simple approximation (the local density approximation) has proved to be enormously successful. Density functional theory (DFT) has been extremely successful over the last thirty years, and is now widely used as a predictive tool in physics, chemistry and materials science [31].

3.1.2. Monte Carlo

Numerical methods that are known as Monte Carlo methods can be loosely described as statistical simulation methods, where statistical simulation is defined in quite general

terms to be any method that utilizes sequences of random numbers to perform the simulation. Monte Carlo methods have been used for centuries, but only in the past several decades has the technique gained the status of a full-fledged numerical method capable of addressing the most complex applications. The name ``Monte Carlo" was coined by Metropolis during the Manhattan Project of World War II, because of the similarity of statistical simulation to games of chance, and the capital of Monaco was a center for gambling and similar pursuits. Monte Carlo is now used routinely in many diverse fields, from the simulation of complex physical phenomena such as radiation transport in the earth's atmosphere and the simulation of the esoteric subnuclear processes in high energy physics experiments, to the mundane, such as the simulation of a Bingo game." The analogy of Monte Carlo methods to games of chance is a good one, but the ``game" is a physical system, and the outcome of the game is not a pot of money or stack of chips (unless simulated) but rather a solution to some problem. The ``winner" is the scientist, who judges the value of his results on their intrinsic worth, rather than the extrinsic worth of his holdings [32].

3.1.3. Molecular Dynamics

One of the principal tools in the theoretical study of biological molecules is the method of molecular dynamics simulations (MD). It's an atomistic simulation method where each atom is treated as a point mass, simple force rules describe the interactions between atoms, Newton's equations are integrated to advance the atomic positions & velocities, and thermodynamic statistics are extracted from the motion of the atoms.

In the broadest sense, molecular dynamics is concerned with molecular motion. Motion is inherent to all chemical processes. Simple vibrations, like bond stretching and angle bending, give rise to IR spectra. Chemical reactions, hormone-receptor binding, and other complex processes are associated with many kinds of intra- and intermolecular motions.

The driving force for chemical processes is described by thermodynamics. The mechanism by which chemical processes occur is described by kinetics. Thermodynamics dictates the energetic relationships between different chemical states, whereas the sequence

or rate of events that occur as molecules transform between their various possible states is described by kinetics.

Energies can be calculated using either molecular mechanics or quantum mechanics methods. Molecular mechanics energies are limited to applications that do not involve drastic changes in electronic structure such as bond making/breaking. Quantum mechanical energies can be used to study dynamic processes involving chemical changes.

Knowledge of the atomic forces and masses can then be used to solve for the positions of each atom along a series of extremely small time steps (on the order of femtoseconds = 10^-15 seconds). First, the atomic accelerations are computed from the forces and masses. The velocities are next calculated from the accelerations. Lastly, the positions are calculated from the velocities. Molecular dynamics has no defined point of termination other than the amount of time that can be practically covered. Unfortunately, the current picosecond order of magnitude limit is often not long enough to follow many kinds of state to state transformations, such as large conformational transitions in proteins.

3.2. Computational Details

3.2.1. Simulation Module: Discover

The calculations were carried out by using the simulation module Discover and forcefield COMPASS in Material Studio of Accelrys Inc. Discover is a molecular simulation program. It provides a broad range of simulation methods; enable to study molecular systems and a variety of materials types. It also makes it possible to perform structural characterization and property prediction for molecules, materials and biological compounds.

Discover incorporates a range of well validated forcefields for dynamics simulations, minimization and conformational searches, allowing you to predict the structure, energetics and properties of organic, inorganic, organometallic and biological systems.

3.2.2. Forcefield

The equilibrium values of bond lengths and angles, plus the force constants, van der Waals radii and associated constants required to calculate the non-bonded interactions, are stored in a file, which is referred to when the energy calculations run. The combination of these parameters with the functional forms of the individual energy terms is known as a forcefield. It is important to appreciate that the ideal values of bonds and angles cannot be based upon element type alone. For example, a carbon-carbon single bond is longer than a carbon-carbon double bond. For this reason, each atom in a structure must have a forcefield type assigned before the energy calculation is run. The forcefield type assigned depends on properties of the atom, such as its hybridization state and environment. The forcefield parameters themselves are stored in the parameter file according to forcefield type.

The results of any mechanics or dynamics calculation depend on the forcefield. The quality of the description of both the system and properties being analyzed is of paramount importance. Choosing the correct forcefield is vitally important in order to get good results from energy calculations.

The potential energy surface: The complete mathematical description of a molecule, including both quantum mechanical and relativistic effects, is a formidable challenge, due to the small scales and large velocities involved. Therefore in the following discussion, these intricacies are ignored. Instead, the focus is on general concepts. This is possible because molecular mechanics and dynamics are based on empirical data that implicitly incorporate all the relativistic and quantum effects.

Since no complete relativistic quantum mechanical theory is suitable for the description of molecules, this discussion starts with the non-relativistic, time-independent form of the Schrödinger description:

$$H\Psi(R,r) = E\Psi(R,r) \tag{3.1}$$

where H is the Hamiltonian for the system, Ψ is the wavefunction, and E is the energy. In general, Ψ is a function of the coordinates of the nuclei (R) and of the electrons (r).

Although the Schrödinger equation is quite general, it is too complex to be of any practical use, so approximations are made. Noting that the electrons are several thousands of times lighter than the nuclei and therefore move much faster, Born and Oppenheimer (1927) proposed the following approximation: the motion of the electrons can be decoupled from that of the nuclei, giving two separate equations. The first of these equations describes the electronic motion:

$$H\Psi(r;R) = E\Psi(r;R) \tag{3.2}$$

and depends only parametrically on the positions of the nuclei. The second equation describes the motion of the nuclei on this potential energy surface $E(R)$:

$$H\Phi(R) = E\Phi(R) \tag{3.3}$$

The direct solution of Equation 3.2 is the province of *ab initio* quantum chemical codes such as Gaussian, CADPAC, Hondo, GAMESS, DMol, and Turbomole. Semiempirical codes such as ZINDO, MNDO, MINDO, MOPAC, and AMPAC also solve Equation 3.2, but they approximate many of the integrals required with empirically fitted functions. The common feature of these programs is that they solve for the electronic wavefunction and energy as a function of nuclear coordinates. In contrast, simulation engines provide an empirical fit to the potential energy surface.

Solving Equation 3.3 is important if you are interested in the structure or time evolution of a model. As written, Equation 3.3 is the Schrödinger equation for the motion of the nuclei on the potential energy surface. In principle, Equation 3.2 could be solved for the potential energy E, and then Equation 3.3 could be solved. However, the effort required to solve Equation 3.2 is extremely large, so usually an empirical fit to the potential energy surface, commonly called a forcefield (V), is used. Since the nuclei are relatively heavy objects, quantum mechanical effects are often insignificant, in which case Equation 3.3 can be replaced by Newton's equation of motion:

$$-\frac{dV}{dR} = m\frac{d^2R}{dt^2} \tag{3.4}$$

The solution of Equation 3.4 using an empirical fit to the potential energy surface $E(R)$ is called molecular dynamics. Molecular mechanics ignores the time evolution of the system and instead focuses on finding particular geometries and their associated energies or other static properties. This includes finding equilibrium structures, transition states, relative energies, and harmonic vibrational frequencies.

The Forcefield: The purpose of a forcefield is to describe the potential energy surface of entire classes of molecules with reasonable accuracy. In a sense, the forcefield extrapolates from the empirical data of the small set of models used to parameterize it, a larger set of related models. Some forcefields aim for high accuracy for a limited set of elements, thus enabling good predictions of many molecular properties. Others aim for the broadest possible coverage of the periodic table, with necessarily lower accuracy.

The forcefield contains all the necessary elements for calculations of energy and force:

- A list of forcefield types
- A list of partial charges
- Forcefield-typing rules
- Functional forms for the components of the energy expression
- Parameters for the function terms
- For some forcefields, rules for generating parameters that have not been explicitly defined
- For some forcefields, a way of assigning functional forms and parameters

The Energy Expression:

The coordinates of a structure combined with a forcefield create an *energy expression (*or *target function*). This energy expression is the equation that describes the potential energy surface of a particular structure as a function of its atomic coordinates. The potential energy of a system can be expressed as a sum of valence (or bond), crossterm, and non-bond interactions:

$$E_{total} = E_{valence} + E_{crossterm} + E_{non-bond} \tag{2.5}$$

The energy of valence interactions is generally accounted for by *diagonal* terms: bond stretching (bond), valence angle bending (angle), dihedral angle torsion (torsion), inversion, also called out-of-plane interactions (oop) terms, which are part of nearly all forcefields for covalent systems, A Urey-Bradley (UB) term may be used to account for interactions between atom pairs involved in 1-3 configurations (i.e., atoms bound to a common atom):

$$E_{valence} = E_{bond} + E_{angle} + E_{torsion} + E_{oop} + E_{UB} \tag{2.6}$$

Modern (second-generation) forcefields generally achieve higher accuracy by including *cross terms* to account for such factors as bond or angle distortions caused by nearby atoms. Crossterms can include the following: stretch-stretch, stretch-bend-stretch, bend-bend, torsion-stretch, torsion-bend-bend, bend-torsion-bend, stretch-torsion-stretch.

The energy of interactions between non-bonded atoms is accounted for by: van der Waals (vdW), electrostatic (Coulomb), hydrogen bond (hbond) terms in some older forcefields.

$$E_{non-bond} = E_{vdW} + E_{Coulomb} + E_{hbond} \tag{2.7}$$

In the corresponding general, summed forcefield function, The forcefield defines the functional form of each term. These are:

- The terms that reflect the energy needed to stretch bonds, bend angles away from their reference values, rotate torsion angles by twisting atoms about the bond axis that determines the torsion angle, distort planar atoms out of the plane formed by the atoms they are bonded to.
- Cross terms that account for interactions between the four types of internal coordinates
- The terms that represent the non-bond interactions as a sum of repulsive and attractive Lennard-Jones terms as well as Coulombic terms, all of which are a function of the distance between atom pairs.

3.2.3. Discover Forcefields

CVFF: The CVFF (consistent-valence forcefield) is a generalized valence forcefield. It was the original forcefield provided with Discover and has been augmented on subsequent releases. CVFF was fitted to small organic (amides, carboxylic acids, etc.) crystals and gas phase structures. It handles peptides, proteins, and a wide range of organic systems. As the default forcefield in Discover, it has been used extensively for many years. It is primarily intended for studies of structures and binding energies, although it also predicts vibrational frequencies and conformational energies reasonably well.

PCFF: The PCFF (Polymer Consistent Forcefield) is intended for application to polymers and organic materials. It is useful for polycarbonates, melamine resins, polysaccharides, other polymers, organic and inorganic materials, about 20 metals, as well as for carbohydrates, lipids, and nucleic acids. PCFF can also be used to calculate cohesive energies, mechanical properties, compressibilities, heat capacities and elastic constants.

COMPASS: COMPASS (Condensed-phase Optimized Molecular Potentials for Atomistic Simulation Studies) is based on the earlier class II CFF9x and PCFF forcefields. In contrast to these earlier forcefields, which were developed with an emphasis on predicting the structure of isolated molecules or pairs of molecules in the gas phase, COMPASS is the first ab initio-based forcefield to have been parameterized using extensive data for molecules in the condensed phase (Sun 1998).

Consequently, COMPASS is able to make accurate predictions of structural, conformational, vibrational, cohesive and thermophysical properties for a broad range of compounds both in isolation and in condensed phases.

Extensive validations have been performed and presented both in the open literature and in Accelrys product tutorials and data sheets. The properties studied include molecular structures and conformational properties (Sun and Rigby, 1997), vibrational frequencies, liquid PVT behavior (Rigby *et al*., 1997), heats of vaporization and solubility parameters (Spyriouni and Vergelati, 2001), crystal cell structures and crystal lattice energies.

3.2.4. Discover Minimization

Minimization is an iterative procedure in which the coordinates of the atoms and possibly the cell parameters, are adjusted so that the total energy of the structure is reduced to a minimum (on the potential energy surface). Minimization results in a structural model which closely resembles the experimentally observed structure. The minimization of a structure is a two step process:

Energy evaluation: The energy expression must be defined and evaluated for a given conformation. Energy expressions which include external restraining terms, to bias the minimization, may be defined in addition to the energy terms.

Conformation adjustment: The conformation is adjusted to reduce the value of the energy expression. A minimum may be found after one adjustment or may require many thousands of iterations, depending on the nature of the algorithm, the form of the energy expression, and the size of the structure.

The efficiency of the minimization is therefore judged by both the time needed to evaluate the energy expression and the number of structural adjustments (iterations) needed to converge to the minimum.

There are several different minimization methods available in Discover. By default, smart minimization is used. This automatically combines appropriate features of the other available methods in a cascade. The Smart Minimizer starts with the steepest descent method, followed by the conjugate gradient method and ends with a Newton method.

Steepest descent: Steepest descent is the method most likely to converge, no matter what the function is or where it begins. It will quickly reduce the energy of the structure during the first few iterations. However, convergence will slow down considerably as the gradient approaches zero. It should be used when the gradients are very large and the configurations are far from the minimum; typically for poorly refined crystallographic data, or for graphically built molecules.

Conjugate gradient: This method improves the line search direction by storing information from the previous iteration. It is the method of choice for systems that are too large for storing and manipulating a second-derivative matrix. The time per iteration is longer than for steepest descents, but this is more than compensated for by efficient convergence. You can choose between Fletcher-Reeves and Polak-Ribiere algorithms.

Newton methods: All the Newton methods require computation and storage of second derivatives and are thus expensive in terms of computer resources. The Newton-Raphson method is only recommended for systems with a maximum of 200 atoms. It has a small convergence radius but it is very efficient near the energy minimum. Discover supports three other variants on the Newton method. The BFGS and DFP quasi-Newton algorithms use an update formula to simulate a second-derivative matrix. Truncated Newton combines the strengths of the conjugate gradient and Newton-Raphson methods.

3.2.5. Structure Preparation

In this work, the systems consisting of a (5,5), (6,6) and (7,7) armchair carbon nanotubes (CNT) were used. These systems are nanotube bundles composed of four armchair nanotubes with different number of hydrogen molecules. For these systems, supercell approach is used. Supercell can be defined as a finite-length slab. Default supercells of nanotubes in Material Studio's structure database were rebuild to a larger supercell for more precise results.

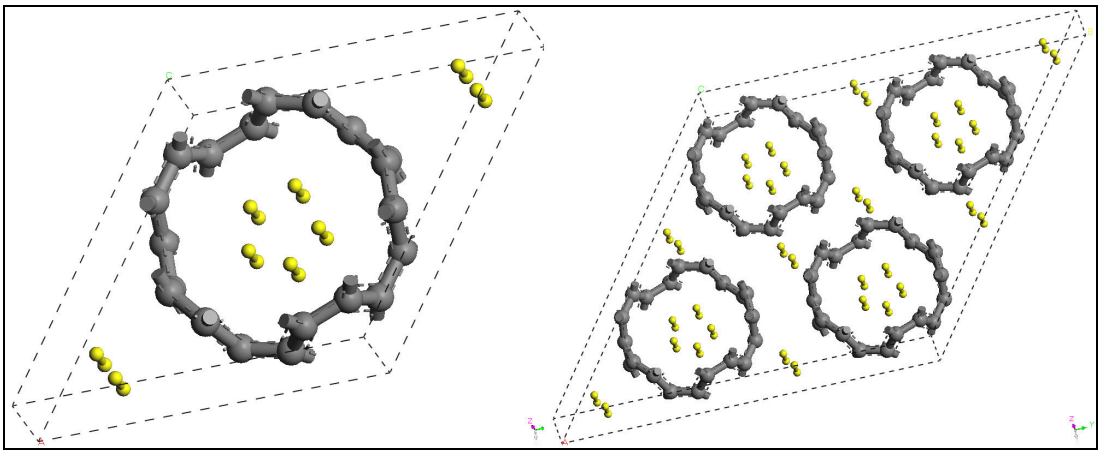

Figure 3.1 Basic supercell and supercell of four nanotubes (5,5 CNT)

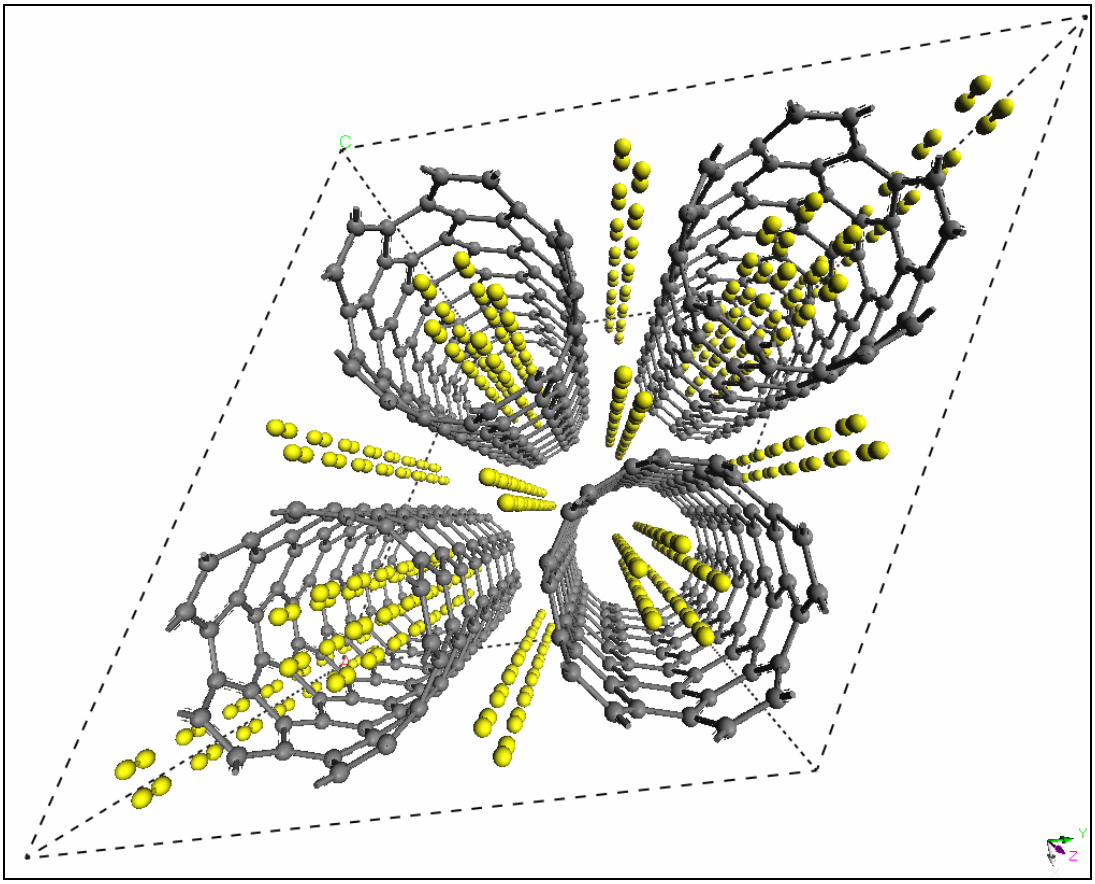

Figure 3.2 Simulation structure with hydrogen molecules (5,5 CNT bundle)

Structure preparation starts from basic one layer carbon nanotube supercell Figure 3.1. Desired amount of hydrogen molecules for inside and outside of nanotube are positioned. Then from this cell with hydrogen molecules, supercell of four nanotubes in triangular array is formed (Figure 3.1) and this supercell is elongated to eight layers to form a final structure to minimization process Figure 3.2. In all systems the hydrogen molecules were placed parallel to the nanotube axis to give the same initial position for minimization for all simulations. Methodology of placing hydrogen molecules for what aim will be explained in Section 4.

3.2.6. Modified Parameters for Simulation

Important parameters that were modified are described in this section.

Forcefield: COMPASS was chosen as a forcefield.

Non bond methods: Non-bond methods and parameters were set for van der Waals and Coulomb interactions

Non-bond cutoff: Calculating non-bond terms can be computationally expensive. To avoid significant increases in calculation times, approximation schemes are often employed. Most simulations use some kind of switching function to smoothly turn off non-bond interactions over a range of distances to a cutoff distance. An effective potential is created by multiplying the actual potential by the smoothing function. Cutoff distance was increase to 15 Å from default value in the simulations.

Minimizer Method: Smart minimizer described previously was chosen and for the Newton method, maximum atom number was increased since the systems are large.

Maximum Iterations: 50000 iterations were set to allow the minimization process to reach a minimum since the systems are large and more iterations can be needed to reach a minimum.

3.2.7. All Discover Setup Parameters with Defaults

Energy Tab:

- Forcefield: COMPASS
- Include Hessian: checked

Non-Bond Tab:

- Apply settings to: vdW and Coulomb
- Summation method: Atom Based
- Quality: Customized
  - Cut-off distance: 15.00
  - Spline width: 3.00
  - Buffer width: 1.00
  - Apply long-range correction: checked

Automation:

- Calculate forcefield types: Conditionally
- Calculate partial charges: Conditionally
- Calculate charge groups: Conditionally

Typing:

- Calculate forcefield types: Conditionally
- Calculate partial charges: Conditionally

Charge groups: Total charge tolerance 0.1 e

3.2.8. All Minimizer Parameters with Defaults

Method: Smart minimizer

- Use steepest descent:
  - Convergence: 1000
  - Line Search: 0.01

- Use Conjugate gradient:
  - Algorithm: Fletcher-Reeves
  - Convergence: 10.0
  - Line search: 0.01

- Use Newton:
  - Algorithm: BFGS
  - Convergence: 1.0e-5
  - Line search: 0.01
  - Maximum atoms: 4000

Convergence Level: Customized

Maximum Iterations: 50000

Optimize cell: checked

4. RESULTS AND DISCUSSION

4.1. Methodology

In the simulations;

- Supercell of carbon nanotube bundles composed of four armchair nanotubes in triangular array as describe in Section 3 were used.
- Calculation parameters were modified for accurate results and for the large system consisting of carbon nanotubes and hydrogen molecules.
- Hydrogen absorption on the walls of nanotubes was neglected. Only physisorption of hydrogen molecules in empty space inside carbon nanotubes and interstitial spaces between nanotubes were accounted.
- (5,5), (6,6) and (7,7) of armchair nanotubes were used to compare the hydrogen absorption on different size of carbon nanotubes.

The simulation methodology for each type of carbon nanotube was below in following order:

- Energy of empty system of carbon nanotube bundle was minimized to have a reference total energy as a comparison basis.
- Simulations were firstly carried out with increasing the number of hydrogen molecules only in the empty space inside of nanotubes to determine favorable amount of hydrogen storage only inside nanotubes. Energy profile of hydrogen loaded nanotube system as a function of the number of hydrogen molecules stored was drawn after sufficient simulations. The system (i.e. nanotube bundle with stored hydrogen) that has a minimum total energy was considered as optimum system and that amount of hydrogen was considered as optimum storage when only inside of the nanotubes were used as the storing media.
- After favorable amount of hydrogen inside carbon nanotubes were found, searching for the system with favorable hydrogen storage was aimed and this time hydrogen molecules were placed also at interstitial spaces between nanotubes. Search for

optimum storage capacity based on the total energy of the system (i.e. nanotube bundle that has stored hydrogen inside the tubes and at the interstitial spaces between nanotubes) were performed for finding optimum total storage capacity and the effect of interstitial storage on the total energy of the system.

- Total hydrogen amount in the system was taken constant and additional simulations were carried out in similar fashion as needed with changing the ratio of hydrogen molecules inside the nanotubes and at the interstitial space between nanotubes. Aim of this procedure was to investigate which type of adsorption, i.e. inner space of nanotubes or the interstitial space between nanotubes, is energetically favorable.
- Simulations with same amount of hydrogen molecules inside space were carried out for (5,5), (6,6) and (7,7) nanotube bundles to compare the hydrogen storage capabilities of these three type of nanotubes.

Total energy of the system consisting of hydrogen molecules in carbon nanotubes is the comparison criteria in this work. Total energy was taken as a direct result from minimization simulations. On the other hand, storage energy of hydrogen molecules in carbon nanotubes was calculated as a difference between the total energy of the system of nanotubes with hydrogen molecules and that of the sum of the energies of its constituent parts:

$$\Delta E = E(CNT - nH_2) - E(CNT) - nE(H_2) \tag{4.1}$$

Since the total energies of the complex and the empty carbon nanotube were known from simulations and the total energy of one hydrogen molecule alone was calculated as zero from simulations, adsorption energy can be simplified to:

$$\Rightarrow \Delta E = E(CNT - nH_2) - E(CNT) \tag{4.2}$$

4.2. (5,5) Armchair Carbon Nanotube

Basic cell of 5,5 carbon nanotube consists of 20 carbon atoms and the number of carbon atoms in its supercell with four armchair nanotubes is 640. Supercell of 5,5

armchair nanotube used in our simulations shown in Figure 4.1. Empty bundle of 5,5 nanotube was simulated and total energy was found as 32542 kcal/mol.

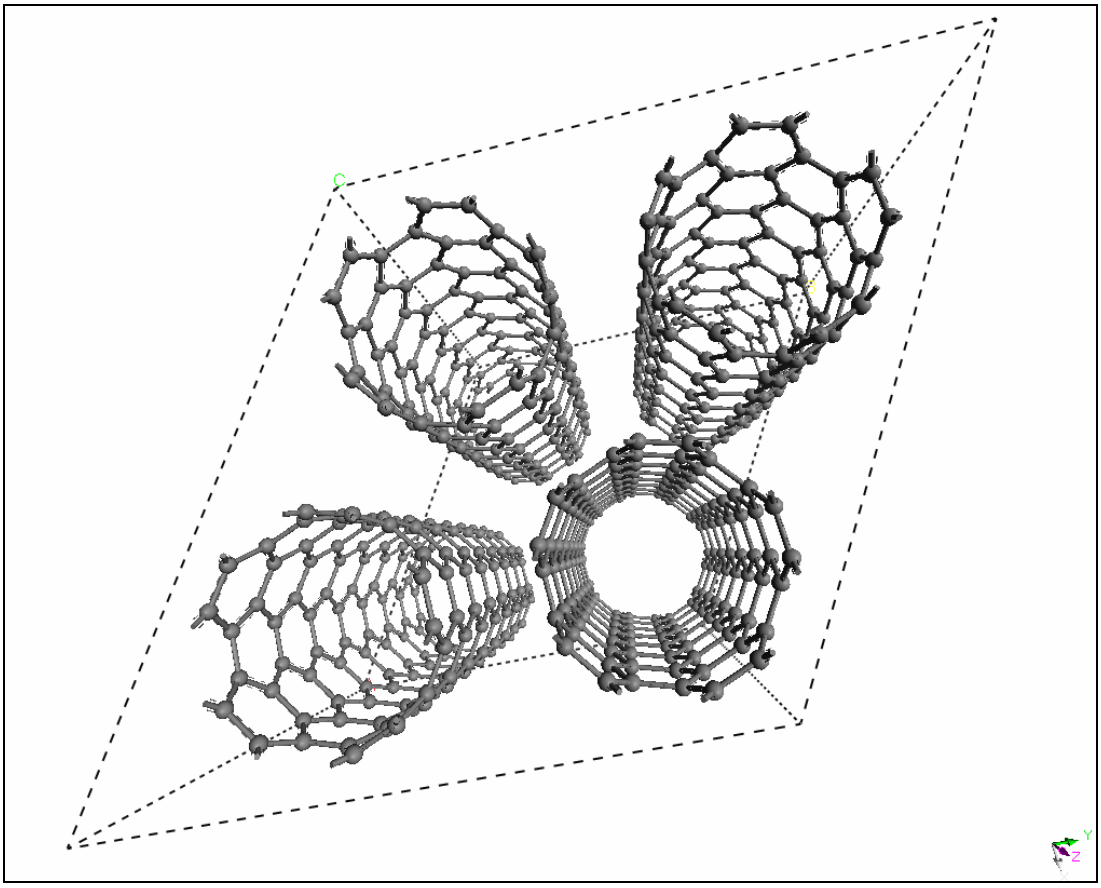

Figure 4.1 Bundle of 5,5 carbon nanotube

4.2.1. Hydrogen Molecules inside the CNT

Simulations with 5,5 armchair nanotubes were followed by only inside loading with hydrogen molecules as mentioned in the methodology. Energy profile was drawn after sufficient simulations as shown in Figure 4.2. For the most favorable amount of hydrogen adsorption, minimum of the graph in Figure 4.2 must be investigated because the lower the energy of the system means more favorable the hydrogen storage inside nanotubes. The system with minimum energy shows that favorable amount of hydrogen inside 5,5 carbon nanotube is 128 molecules. It correspond to a 2.44 wt. per cent of hydrogen storage and a load of 0.4. Load is defined as the ratio of number of hydrogen atoms to the number carbon atoms in the complex.

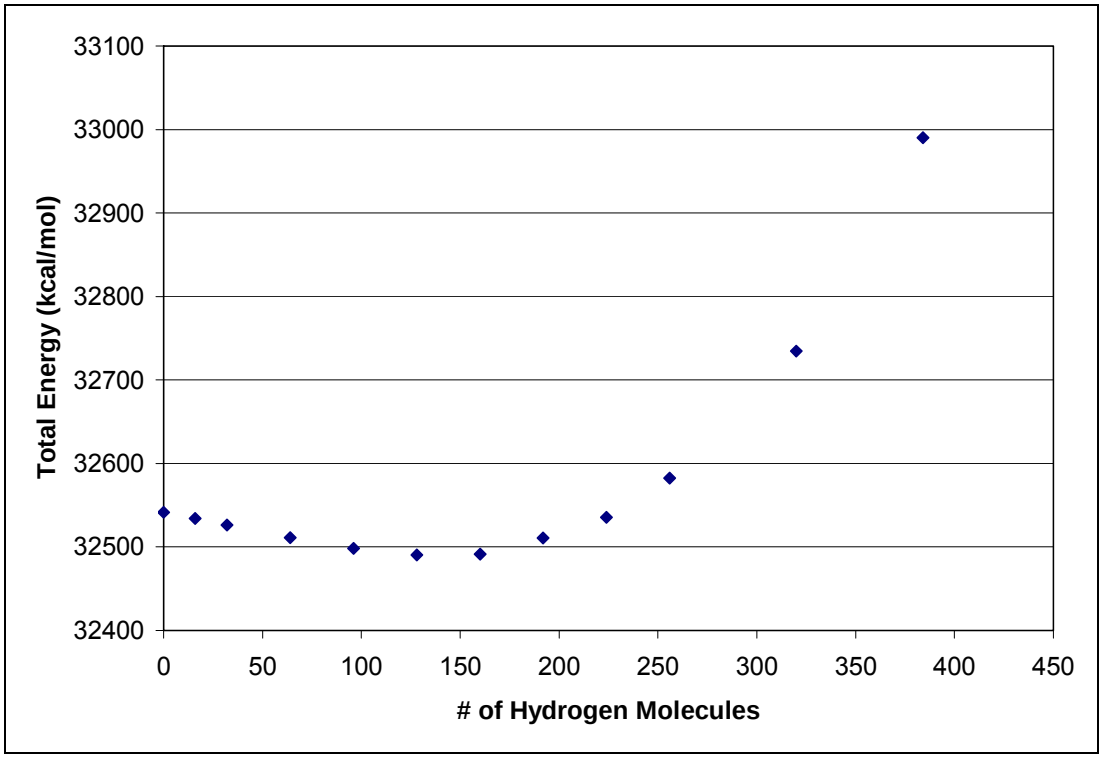

Figure 4.2 Energy change with respect to # of hydrogen molecules inside of 5,5 CNT

Figure 4.3 shows top and the corresponding side views of minimized 5,5 carbon nanotube bundle with 128 hydrogen molecules inside. Due to narrow diameter of the nanotube and the strong van der Waals forces at short distance between hydrogen molecules in the tubes, hydrogen molecules condense to a molecular shell with tube shape as shown in Figure 4.3. It should be noted that this shape was changed to a cylindrical block with higher number of hydrogen molecules stored inside.

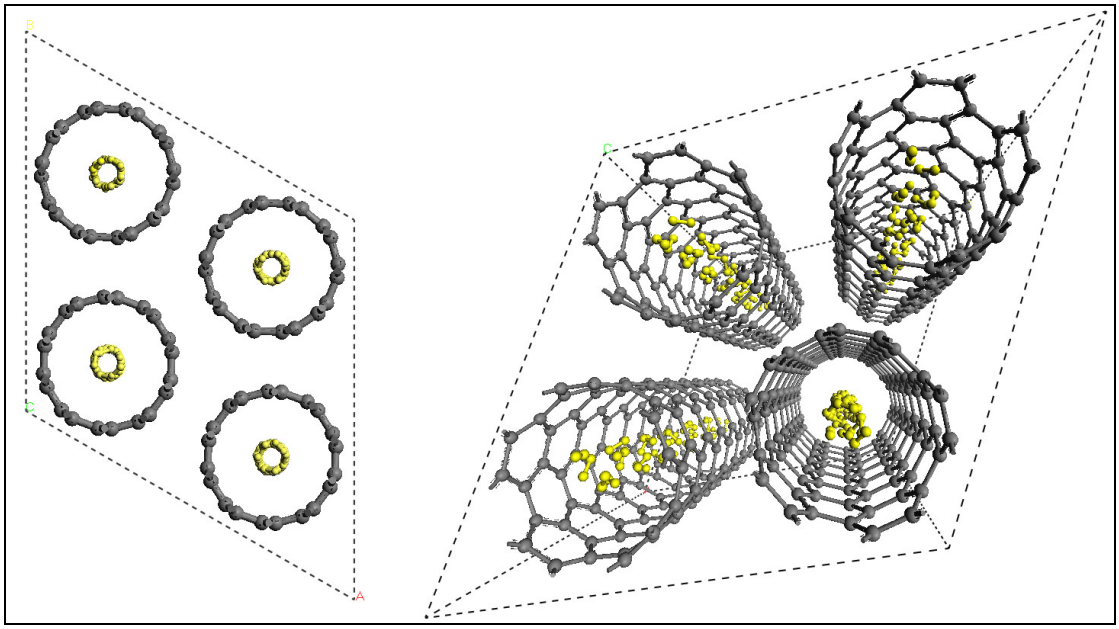

Figure 4.3 Top and side views of 5,5 CNT bundle with 128 hydrogen molecules.

4.2.2. Hydrogen Molecules at Interstitial Space between Nanotubes

The system of carbon nanotube bundles composed of four armchair nanotubes gives an opportunity to test whether the interstitial spaces between nanotubes are favorable for hydrogen storage or not. For this purpose, the system with optimum hydrogen storage by only inside loading was taken and this time, simulations were carried out with increasing the hydrogen molecules at interstitial space between nanotubes while keeping the number of hydrogen molecules inside the nanotubes fixed. Additional simulations were run on the system with 320 hydrogen molecules inside nanotubes, which is not stable according to only inside storage of hydrogen simulations, for further investigation of hydrogen storage at interstitial spaces.

In the first system which has optimum inside loading total energy profiles are shown in Figure 4.4. Adding even small number of hydrogen at interstitial space between nanotubes has an effect of sharp increase on total potential energy of the system. Energy profile changes for 192, 256 and 320 hydrogen molecules at interstitial space. The possible reason might be that; large amount of hydrogen molecules at interstitial space increased the intertube distance between nanotubes which may result in to a decrease in van der Waals forces that led to low total potential energy values. Although energy profile changes of the

system for this interval shows that the system is still not stable as in the initial case, the energy profile keeps increasing after 320 interstitial hydrogen molecules.

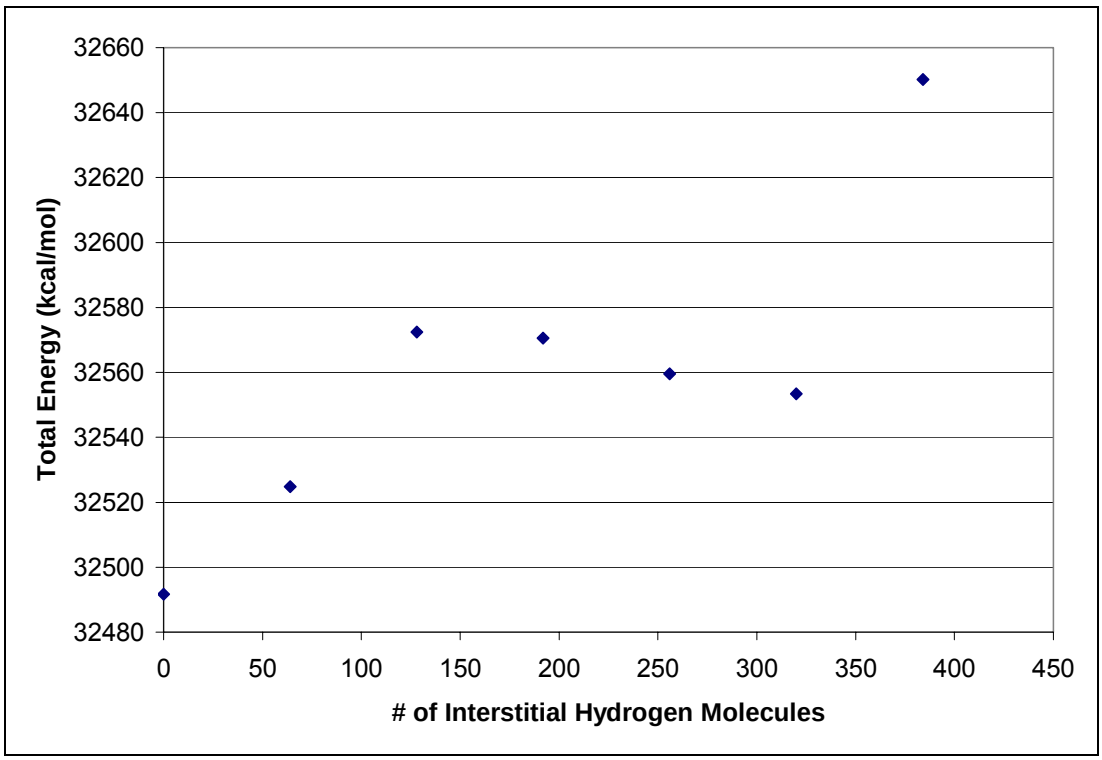

Figure 4.4 Energy change with 160 hydrogen molecules fixed inside (5,5 CNT)

Total energy of second test system (which has 320 hydrogen molecules inside) increases with adding more hydrogen molecules at interstitial space between nanotubes as shown in Figure 4.5. Energy of the system gradually increases at the beginning but then a sudden increase occur after one point, i.e. 64 hydrogen molecules at the interstitial area, and this can be again related to an increase in the intertube distance. Adding hydrogen molecules at interstitial spaces on second system show no stable form as in the first system.

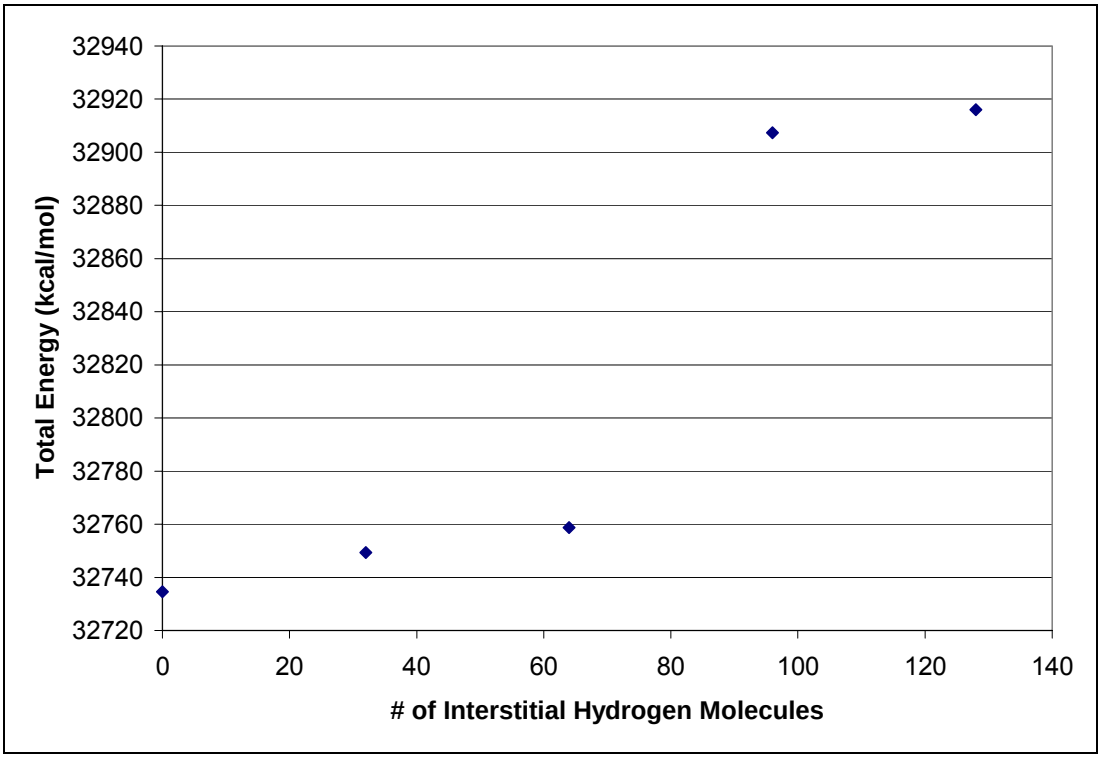

Figure 4.5 Energy change with 320 hydrogen molecules fixed inside (5,5 CNT)

4.2.3. Fixed Total Amount of Hydrogen Molecules at Different Sites

Additional simulations were run with fixed amount of hydrogen molecules with different portions inside and at interstitial space, aiming to furtherly study the favorability of storing hydrogen molecules at interstitial space between nanotubes. Other aim of these simulations was to find a best ratio of hydrogen molecules inside to hydrogen molecules at interstitial spaces for hydrogen storage (or at least to check whether there exist an optimum ratio). Table 4.1 summarizes the results for 160, 224 and 320 fixed amount of hydrogen molecules.

The system consists of 160 hydrogen molecules inside the empty space in the nanotubes is close to optimum storage as mentioned above. Transferring 64 hydrogen molecules (40 per cent) from inner part of the nanotubes to interstitial space increases the total energy of the system. Therefore, only inside storage is most stable state for 160 hydrogen molecules.

Table 4.1 Fixed total amount of hydrogen molecules at different sites (5,5 CNT)

H_2 Inside Nanotubes	H_2 at Interstitial Space	Total H_2	Energy (kcal/mol)
160	0	160	32492
96	64	160	32531
224	0	224	32536
160	64	224	32525
320	0	320	32735
256	64	320	32616
192	128	320	32597

Other system to be investigated was the bundle with only inside loading of 224 hydrogen molecules. If 64 hydrogen molecules of inside molecules loaded at interstitial space, total potential energy decreases slightly. Since 224 hydrogen molecules inside nanotubes higher than the favorable amount of hydrogen storage only inside the empty space in the nanotubes, storing the same amount with small portion at interstitial space decreased the hydrogen molecules inside the nanotubes, which led to a lowering of the van der Waals forces between very close hydrogen molecules.

320 hydrogen molecules is a very large number to be stored inside nanotubes for the supercell used in the simulations. Large number of hydrogen molecules exerts strong van der Waals forces to each others and to the nanotube wall from the inside due to narrow diameter of nanotube and, as found in simulations potential energy of the system with 320 hydrogen molecules inside, the system was not stable. Storage of same amount with interstitial hydrogen molecules lowers the potential energy but the values are still far from favorable state , showing that storage of that amount hydrogen (5.9 wt. per cent and load of 1.0) on 5,5 nanotubes is not possible in stable form.

4.2.4. Optimum Hydrogen Storage in (5,5) Carbon Nanotube

The results and above discussions show that hydrogen storage on 5,5 armchair nanotubes is favorable for only hydrogen molecules inside the empty space of nanotubes. Therefore, optimum hydrogen storage in (5,5) carbon nanotubes was found as 2.44 wt. per cent of hydrogen storage and load of 0.4 with only inside loading of hydrogen.

Other works on 5,5 carbon nanotubes are in line with this result. Ma *et al*. [33, 24] found similar results in their molecular dynamics works. Their calculations were performed for 5,5 single wall nanotubes and every end of the tubes were capped by hemi sphere of fullerene with inside loading of hydrogen. In earlier study [33], they stored 90 hydrogen atoms in 5,5 single wall nanotube which consists of 150 carbon atoms corresponding to 3.6 wt. per cent of hydrogen storage and load of 0.6. In latter work [24], single wall nanotubes with 210 carbon atoms were used and they found that defined 5,5 single wall nanotube capsules can accommodate 43 hydrogen molecules, at most. The weight efficiency is about 2.5% and the load is 0.41. Our calculations are in agreement with these results.

However, Lee *et al*. [3] reached a much higher hydrogen storage in 5,5 carbon nanotubes, load of 1.2 corresponds to 7 wt. per cent hydrogen. This study is unfortunately somewhat misleading. The authors use electronic density functional theory and a tight-binding formalism to study the geometry and chemical binding properties of atomic hydrogen inside and outside of an isolated single wall carbon nanotube. Tight binding studies can be very useful for chemically bonded species, but they do not give any information on long-range electron correlation, which is responsible for the physisorption phenomenon. Notably, the study indicates that chemisorption of atomic hydrogen on each carbon atom inside a nanotube is energetically unstable. The system relaxes to form molecular hydrogen inside the nanotube. Although this study gives unrealistic results, this behavior supports our decision of choosing molecular dynamics method as our calculation scheme.

These studies on hydrogen storage on carbon nanotubes also show same hydrogen shell forming inside 5,5 and other size of carbon nanotubes as seen in Figure 4.3.

4.3. (6,6) Armchair Carbon Nanotube

Basic cell of 6,6 carbon nanotube consists of 24 carbon atoms and the number of carbon atoms in its supercell with four armchair nanotubes is 768. Supercell of 6,6 armchair nanotube used in the simulations shown in Figure 4.9. Empty bundle of 6,6 nanotube was simulated and total energy was found as 38905 kcal/mol.

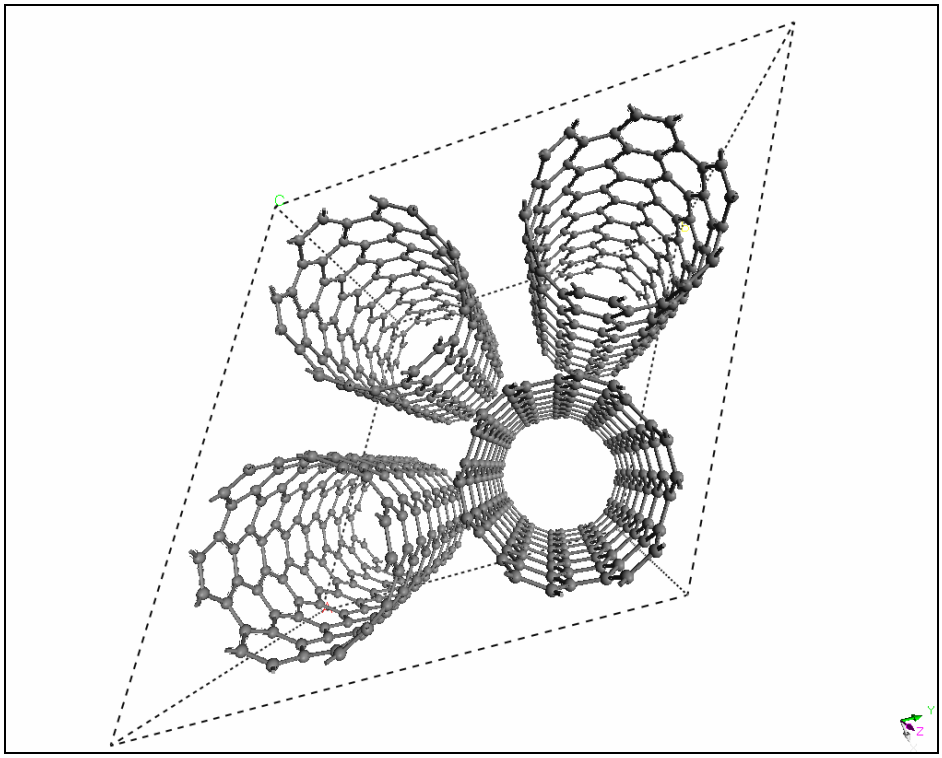

Figure 4.6 Bundle of 6,6 carbon nanotube

4.3.1. Hydrogen Molecules inside the CNT

As the simulations with 5,5 armchair nanotubes, 6,6 armchair nanotube calculations were also started with same procedure; only inside loading with hydrogen molecules. For the 6,6 nanotube bundle, most favorable amount of hydrogen storage can be determined from the stored hydrogen amount that gave a total minimum energy for the system. Minimum total energy shows that favorable amount of hydrogen inside 6,6 carbon nanotube is 320 hydrogen molecules. It correspond to a 5 wt. per cent of hydrogen storage and a load of 0.83.

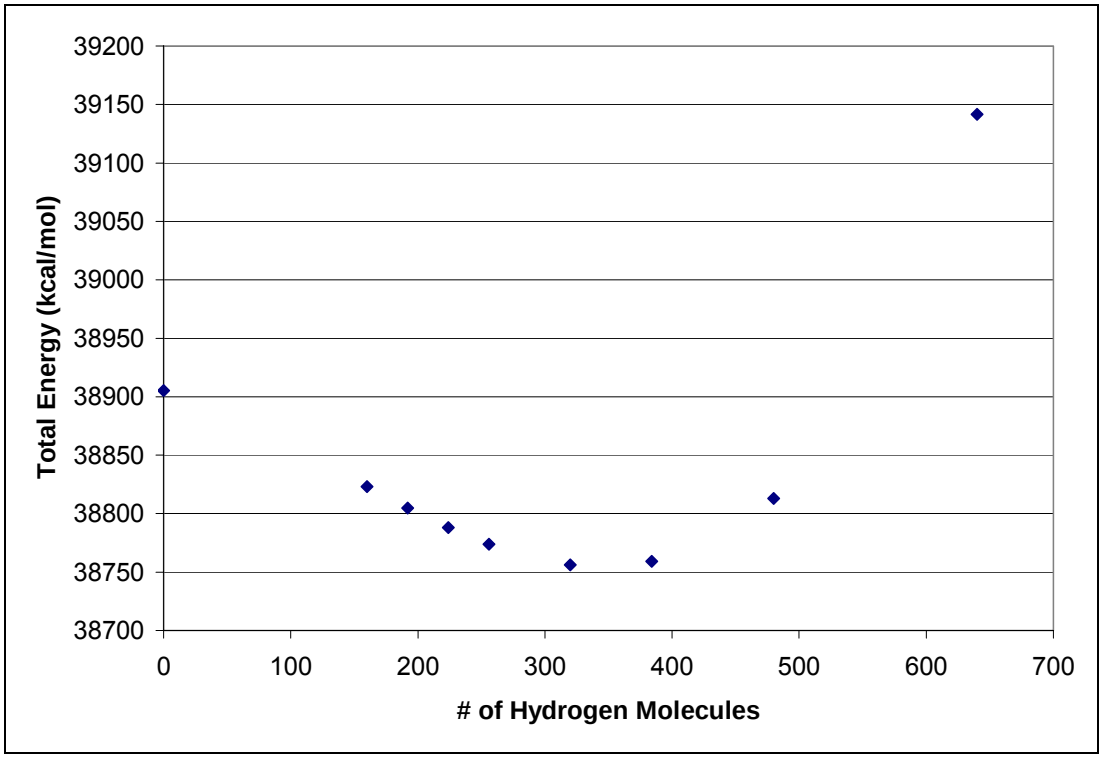

Figure 4.7 Energy change with respect to # of hydrogen molecules inside of 6,6 CNT

From the results for 6,6 carbon nanotubes mentioned above, it is found that 6,6 nanotube bundle have higher hydrogen storage capacity inside nanotubes than 5,5 nanotube bundle. This can be related to diameter of nanotubes. Since the diameter of 6,6 nanotube is larger than the diameter of 5,5 nanotube, it has larger space for hydrogen molecules. Thus, higher amount of hydrogen molecules can be stored in 6,6 nanotube before van der Waals forces became a problem.

Same tendency of forming a molecular shell also observed in supercell of 6,6 carbon nanotubes as shown in Figure 4.8.

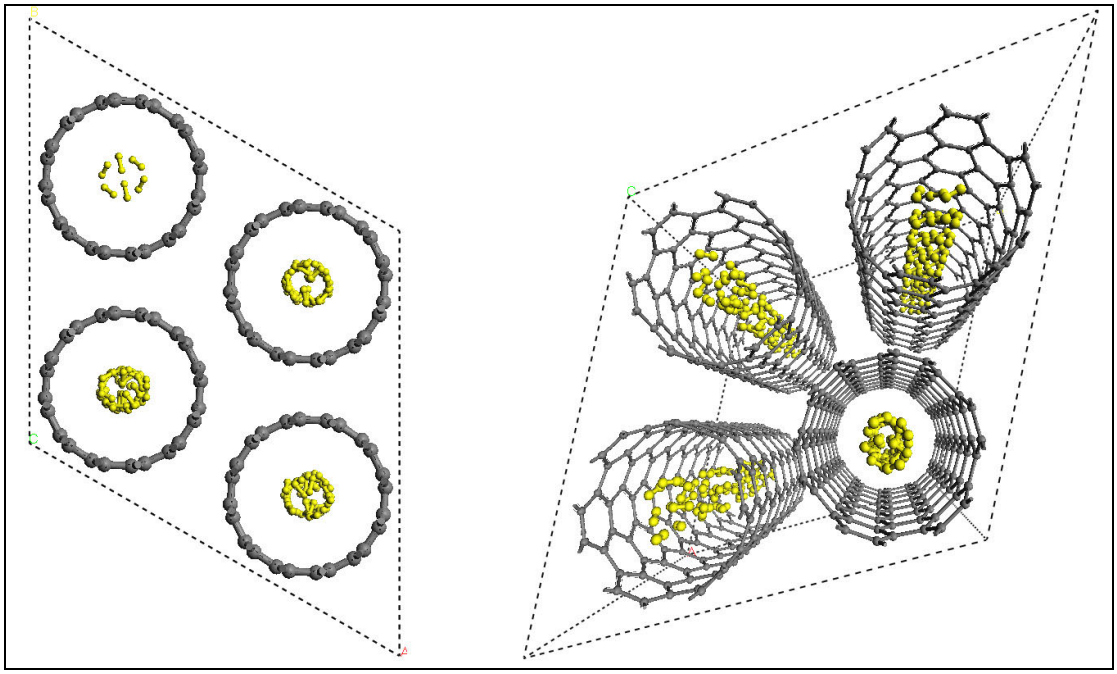

Figure 4.8 Top and side views of 6,6 CNT with 192 hydrogen molecules

4.3.2. Hydrogen Molecules at Interstitial Space between Nanotubes

Favorability of the interstitial spaces between 6,6 nanotubes for storing hydrogen was also studied in supercell of 6,6 carbon nanotubes. Three comparison can be made from the simulations run with 6,6 carbon nanotube bundles with optimum hydrogen loading of 320 molecules and for additional systems with hydrogen loading of 192 and 256 hydrogen molecules.

Supercell of carbon nanotubes with 192 hydrogen molecules inside nanotubes has less hydrogen molecules than most favorable result with only inside hydrogen loading. Adding hydrogen molecules at interstitial space of this supercell increases the total potential energy as in Figure 4.9. Although this supercell is stable enough even after addition of small number of hydrogen molecules at interstitial spaces, there was increase in the energy of the system and therefore, storing hydrogen at the interstitial spaces of this system was found not favorable.

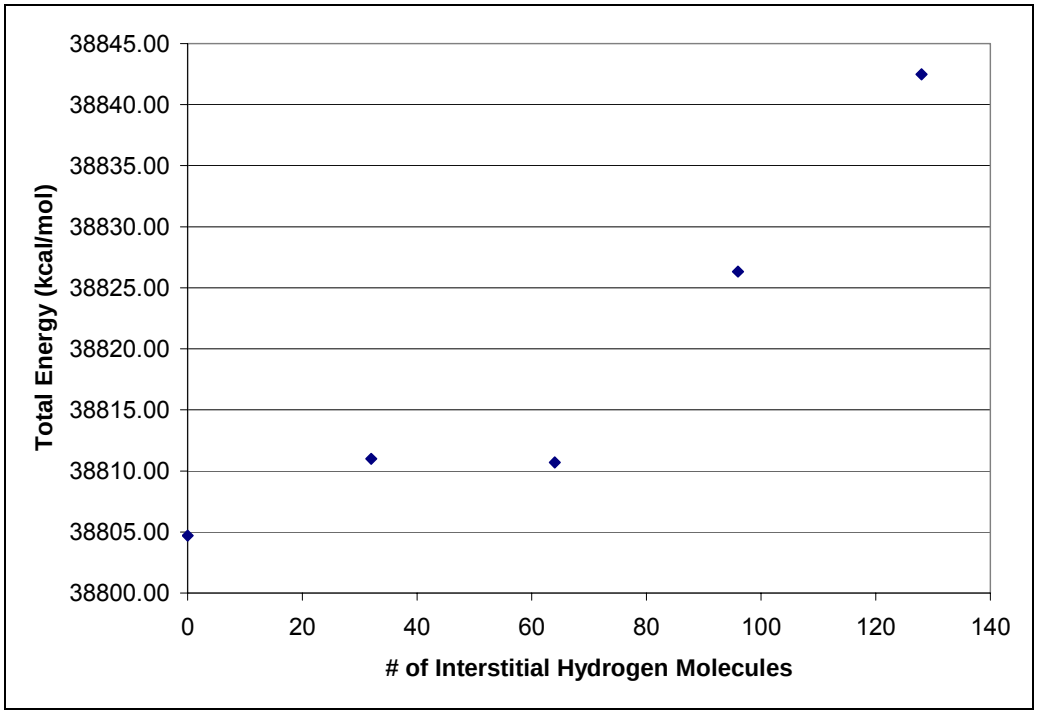

Figure 4.9 Energy change with 192 hydrogen molecules fixed inside (6,6 CNT)

Table 4.2 and 4.3 show the relation between the total energy and interstitial hydrogen addition where inside loading were kept fixed at 256 and 320 hydrogen molecules, respectively. 5,5 nanotube bundle with larger hydrogen amount stored inside gives controversial results with this procedure but, it is clearly seen from the results of supercell of 6,6 nanotubes that storing hydrogen at the interstitial space of 6,6 carbon nanotube bundle is not favorable.

Table 4.2 Energy changes with 256 hydrogen molecules fixed inside (6,6 CNT)

H_2 Inside Nanotubes	H_2 at Interstitial Space	Total H_2 Molecule	Energy (kcal/mol)
256	0	256	38773.73
256	64	320	38778.37
256	128	384	38810.60

Table 4.3 Energy change with 320 hydrogen molecules fixed inside (6,6 CNT)

H_2 Inside Nanotubes	H_2 at Interstitial Space	Total H_2 Molecule	Energy (kcal/mol)
320	0	320	38756.18
320	64	384	38761.11
320	128	448	38791.00

4.3.3. Fixed Total Amount of Hydrogen Molecules at Different Sites

Hydrogen storage favorability of empty space inside nanotubes and interstitial space between nanotubes in bundle were further studied with fixed total amount of hydrogen molecules with different portions inside and at interstitial space.

There is not much to discuss for 6,6 nanotubes in this section as in 5,5 nanotubes since transferring some portion of hydrogen molecules inside nanotubes to interstitial space between nanotubes increases total energy for all inside loading levels of hydrogen molecules tested (224, 320 and 384 hydrogen molecules) as given in Table 4.4. This can be related to the larger diameter of 6,6 nanotube compared to that of 5,5 nanotube. Thus, the empty space inside 6,6 carbon nanotubes was found more favorable than interstitial space between nanotube in the bundle.

Table 4.4 Fixed total amount of hydrogen molecules at different sites (6,6 CNT)

H2 Inside Nanotubes	H2 at Interstitial Space	Total H2 Molecule	Energy (kcal/mol)
224	0	224	38788.03
192	32	224	38810.98
160	64	224	38828.54
320	0	320	38756.18
256	64	320	38778.37
192	128	320	38842.49
384	0	384	38759.07
320	64	384	38761.11
256	128	384	38810.60

4.3.4. Optimum Hydrogen Storage in (6,6) Carbon Nanotube

The results and above discussions show that hydrogen storage on 6,6 armchair nanotubes is similar to 5,5 carbon nanotubes; only inside loading of hydrogen molecules is more favorable than that at interstitial spaces. Therefore, the optimum hydrogen storage in (6,6) carbon nanotubes was found as 5 wt. per cent of hydrogen storage and load of 0.83.

4.4. (7,7) Armchair Carbon Nanotube

Basic cell of 7,7 carbon nanotube consists of 28 carbon atoms and the number of carbon atoms in its supercell with four armchair nanotubes is 896. Supercell of 7,7 armchair nanotube used in our simulations shown in Figure 4.10. Empty bundle of 6,6 nanotube was simulated and total energy was found as 45298 kcal/mol.

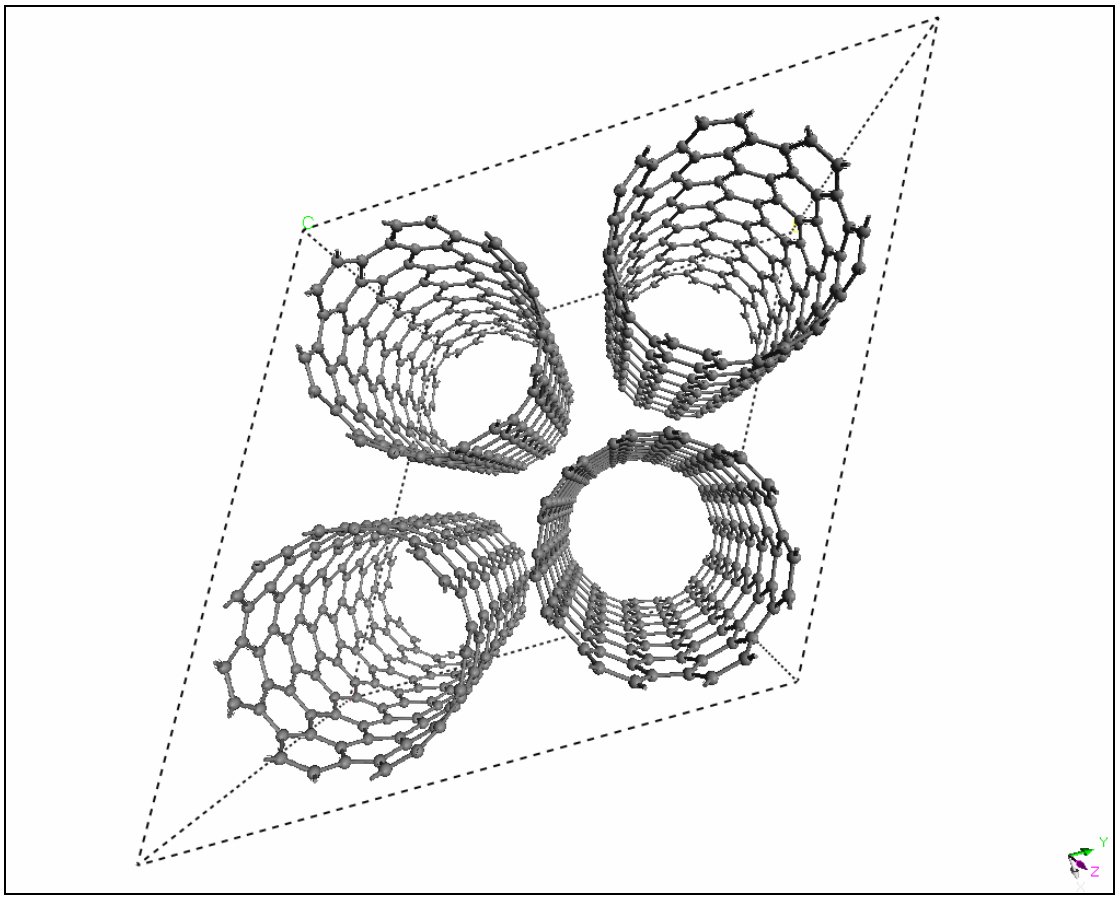

Figure 4.10 Bundle of 7,7 carbon nanotube

4.4.1. Hydrogen Molecules inside the CNT

Results and discussion about only inside loading of 7,7 carbon nanotube bundles with hydrogen molecules is given in this section. Since 7,7 armchair nanotubes have largest diameter among the nanotubes used in our work, it is expected that its hydrogen storage capacity should be higher than others. Most favorable amount of hydrogen storage can be determined from the hydrogen loading level that gave the minimum energy. The minimum of the total energy (Figure 4.11) indicates that favorable amount of hydrogen

inside 7,7 carbon nanotube is 640 hydrogen molecules. It correspond to a 8.2 wt. per cent of hydrogen storage and a load of 1.43.

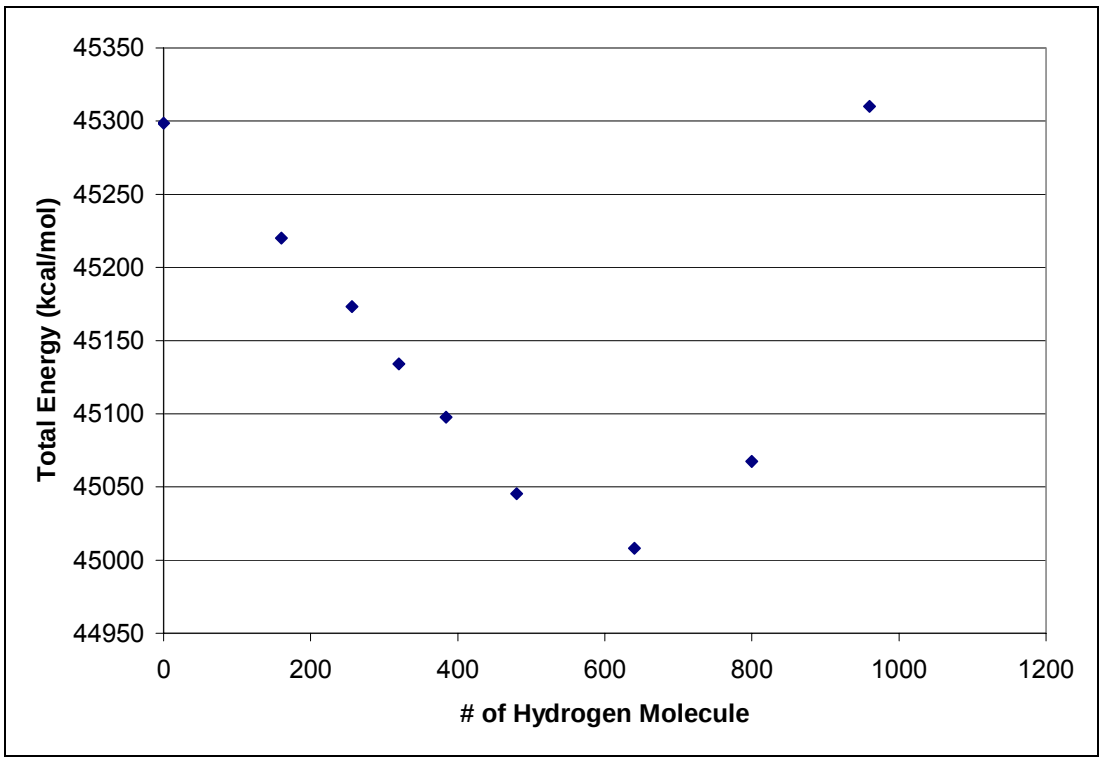

Figure 4.11 Energy change with respect to # of hydrogen molecules inside of 7,7 CNT

As mentioned before the hydrogen absorption capability of 7,7 carbon nanotube was found higher than 5,5 and 6,6 carbon nanotubes as expected due to its larger diameter and the larger empty space inside (7,7) nanotubes.

Figure 4.12 shows top and the corresponding side views of minimized 7,7 carbon nanotube bundle with 640 hydrogen molecules inside. Same tendency of forming a shell also observed in supercell of 6,6 carbon nanotubes but this time the shape changed to a cylindrical block due to a higher number of hydrogen molecules inside.

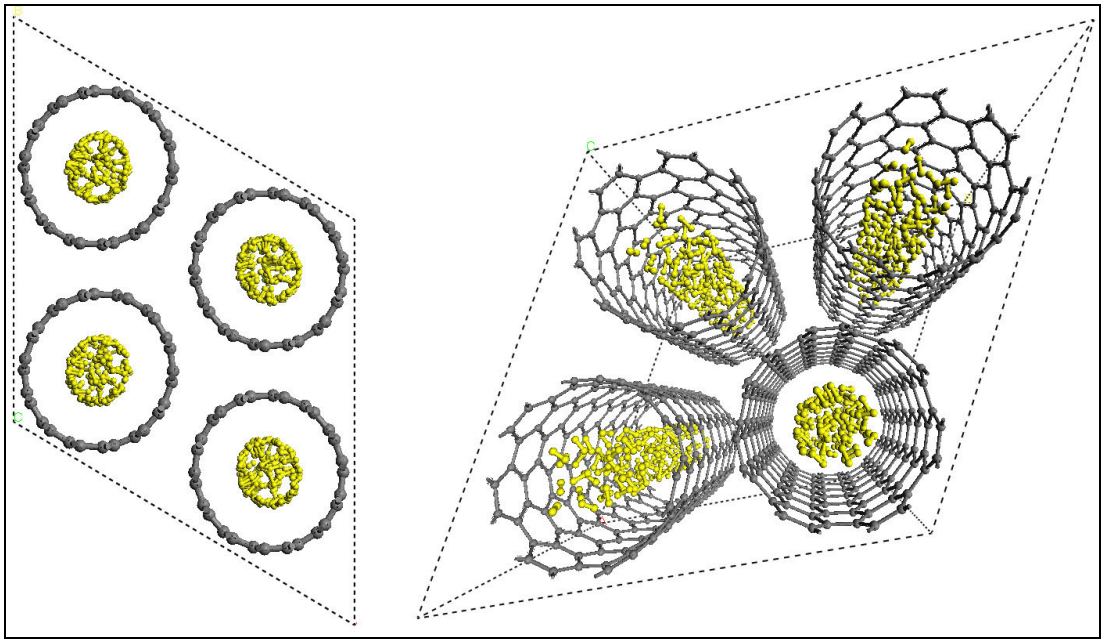

Figure 4.12 Top and side views of 7,7 CNT bundle with 640 hydrogen molecules.

4.4.2. Hydrogen Molecules at Interstitial Space between Nanotubes

The Simulation results used for investigating the hydrogen storage favorability of interstitial space between nanotubes were tabulated in Table 4.5. The comparisons indicate that the result is same as in 6,6 carbon nanotubes; interstitial spaces inside 7,7 carbon nanotube bundles are not favorable for hydrogen storage. All comparisons show that adding hydrogen molecules at interstitial spaces of carbon nanotube bundle, which were initially loaded with hydrogen molecules inside, increases the energy of the system, showing that interstitial space is not favorable hydrogen storage sites for 7,7 nanotubes.

Table 4.5 Energy changes with hydrogen molecules fixed inside (7,7 CNT)

H2 Inside Nanotubes	H2 at Interstitial Space	Total H2	Energy (kcal/mol)
160	0	160	45220
160	64	224	45225
256	0	256	45173
256	128	384	45187
320	0	320	45134
320	64	384	45139
384	0	384	45098
384	64	448	45105

4.4.3. Fixed Total Amount of Hydrogen Molecules at Different Sites

Hydrogen storage favorability of empty space inside nanotubes and interstitial space between nanotube bundle were further studied with same amount of hydrogen molecules with different portions distributed inside and at interstitial space but nothing different from 6,6 nanotubes simulations are expected since 7,7 carbon nanotubes have largest diameter in nanotubes used and have larger empty space inside nanotubes accordingly to store hydrogen molecules inside nanotubes. Thus, empty space inside nanotube becomes more favorable site than interstitial space between nanotube bundle. Table 4.6 shows the simulations results which support this discussion.

Table 4.6 Fixed total amount of hydrogen molecules at different sites (7,7 CNT)

H2 Inside Nanotubes	H2 at Interstitial Space	Total H2	Energy (kcal/mol)
384	0	384	45098
320	64	384	45133
256	128	384	45187
640	0	640	45008
576	64	640	45019
512	128	640	45055

As a general result, empty space inside nanotubes gets more favorable than interstitial spaces as the diameter of nanotubes in bundle increases

4.4.4. Optimum Hydrogen Storage in (7,7) Carbon Nanotube

The results of the simulations of hydrogen storage on 7,7 armchair nanotubes showed that only inside loading of hydrogen molecules is more favorable than interstitial spaces as former results with 5,5 and 6,6 nanotubes. Therefore, the optimum hydrogen storage in (7,7) carbon nanotubes was found as 8.2 wt. per cent of hydrogen storage and a load of 1.43.

4.5. Comparison of Hydrogen Storage of Different Carbon Nanotubes

Main object of this work is to compare the hydrogen storage capabilities of different sized carbon nanotubes and to find the effect of nanotube size on hydrogen storage capacity. To reach that object dozens of simulations were carried out on (5,5), (6,6) and (7,7) nanotube bundles. Since the discussions so far have showed that hydrogen storage at interstitial spaces between nanotubes is not favorable, in this section, effect of nanotube size on hydrogen storage will be only discussed for inside loading of hydrogen.

One way of comparison is through the energy difference of hydrogen storage per carbon atom. By this way, storage of the same number of hydrogen molecules inside different nanotubes can be investigated and the size effect of the nanotube on storage can be discussed. The energy difference per carbon atom is calculated by enhancing the Equation 4.2;

$$\Delta E / Carbon\ atom = \left[E(CNT - nH_2) - E(CNT)\right]/(No.of\ \ Carbon\ atoms) \qquad (4.3)$$

All the simulation results are presented in Figure 4.13 as “Energy/carbon” vs “# of hydrogen molecules stored”. Energy difference per carbon atom with varying the number of hydrogen molecules inside nanotubes in bundles of (5,5), (6,6) and (7,7) were given in Figure 4.13. When the minimum of the curves are compared, 5,5 carbon nanotube bundle is found stable with smallest amount of hydrogen molecule stored while 7,7 carbon nanotube bundle has the maximum amount of hydrogen stored inside. Additionally, 7,7 carbon nanotube have the lower adsorption energy per carbon atom at its optimum hydrogen load. These results show that 7,7 carbon nanotube bundle is capable of storing higher amount of hydrogen molecules inside the nanotubes and the storage is more stable than the others at the favorable hydrogen storage levels.

Studies of Ma *et al*. [24] and Lee *et al*. [3] also shows the same trend that hydrogen storage inside nanotubes increases as the size of nanotube increase. Both studies worked on (5,5) and (10,10) carbon nanotubes. Their calculation methods were different but the conclusion on nanotube size they reach was the same, although in their papers, the given amounts of hydrogen storage are different.

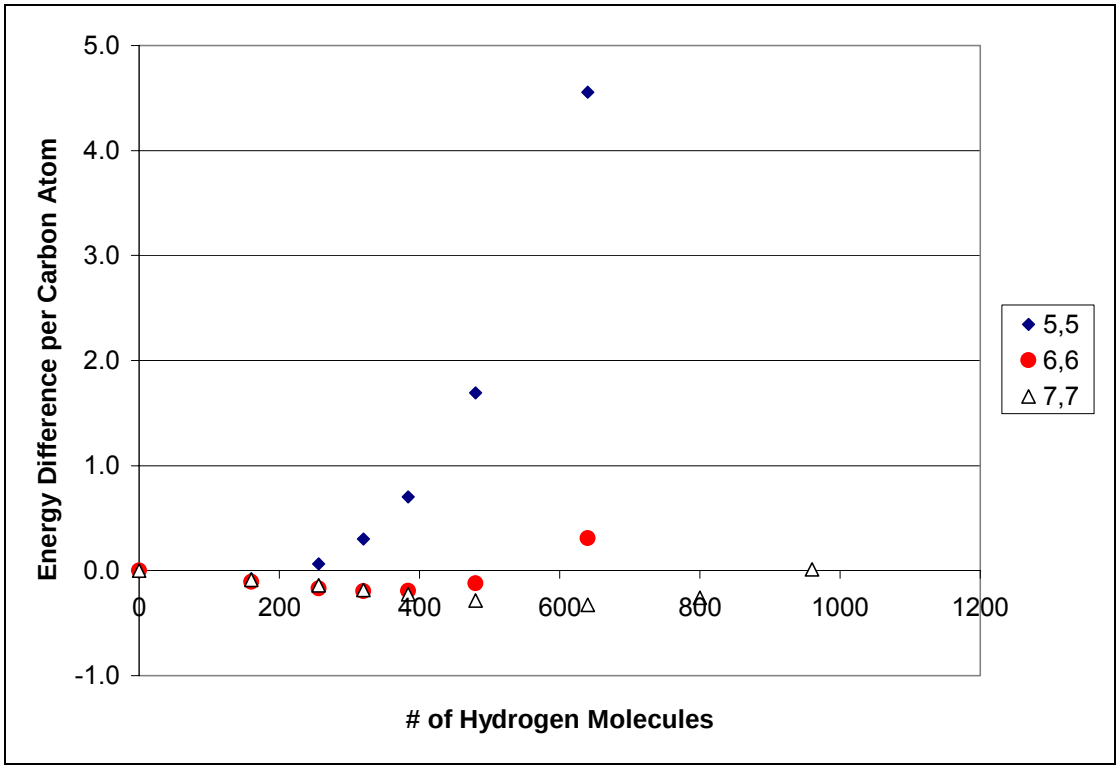

Figure 4.13 Energy difference per carbon atom vs. # of hydrogen molecules

So far, hydrogen storage based on minimum of total energy of system has been studied. Other comparison criteria could be energy difference per hydrogen molecule; thus, the storage of same amount of hydrogen molecules at different size of nanotubes can be examined. Storage energy difference per carbon atom is calculated by enhancing the Equation 4.2;

$$\Delta E / H_2 = \left[E(CNT - nH_2) - E(CNT)\right] / (No.of\ H_2) \tag{4.4}$$

Figures 4.14-16 show storage energy difference per hydrogen molecule with respect to number of hydrogen molecules for different carbon nanotubes used. If the minimum of graphs were taken as favorable hydrogen storage by storage energy difference per hydrogen molecules, Table 4.8 can be constructed for nanotubes used. Table 4.7 show the hydrogen storage values based on total energy that were found so far.

Table 4.7 Storage data of CNTs based on total energy

	wt.% of H2	Load (H/C)
5,5 CNT	2.44	0.40
6,6 CNT	5.00	0.83
7,7 CNT	8.20	1.43

Table 4.8 Storage data based on energy difference per hydrogen molecule

	wt.% of H2	Load (H/C)
5,5 CNT	1.23	0.20
6,6 CNT	3.03	0.50
7,7 CNT	6.28	1.07

To estimate the storage capacity, hydrogen density was assumed to be nearly constant inside the tube. The volume and the number of the hydrogen atoms increases with a square of the radius, whereas the number of carbon atoms increases linearly with the radius. Therefore, it is expected that hydrogen storage capacity should be linearly proportional to the radius or diameter. If the hydrogen storage values for two cases, Table 4.7 and 4.8, graphed with respect to diameter of nanotubes, linear lines are formed as in Figure 4.17.

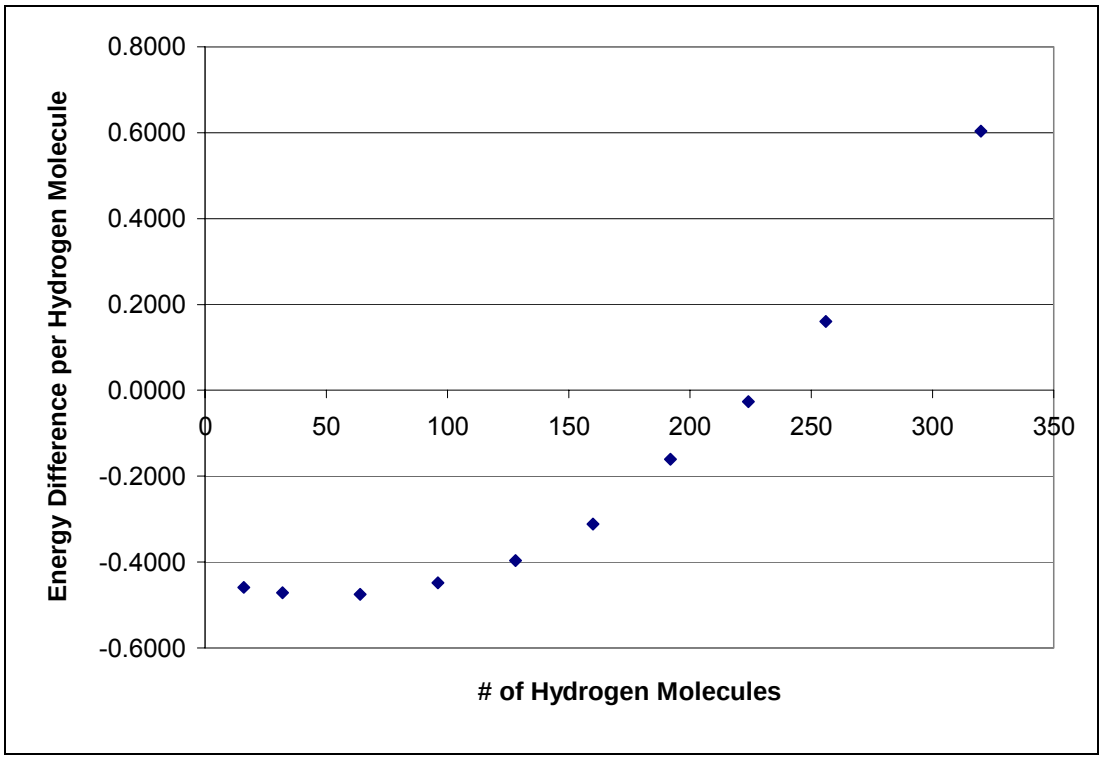

Figure 4.14 Energy difference per H_2 in 5,5 CNT

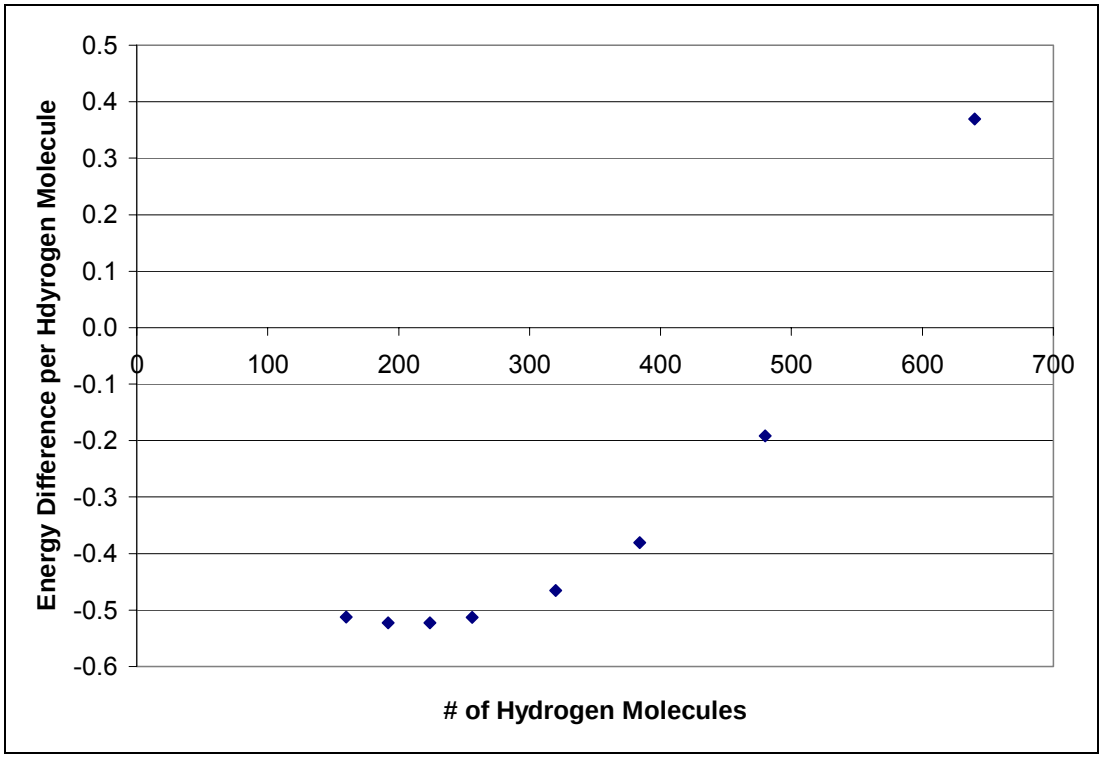

Figure 4.15 Energy difference per H_2 in 6,6 CNT

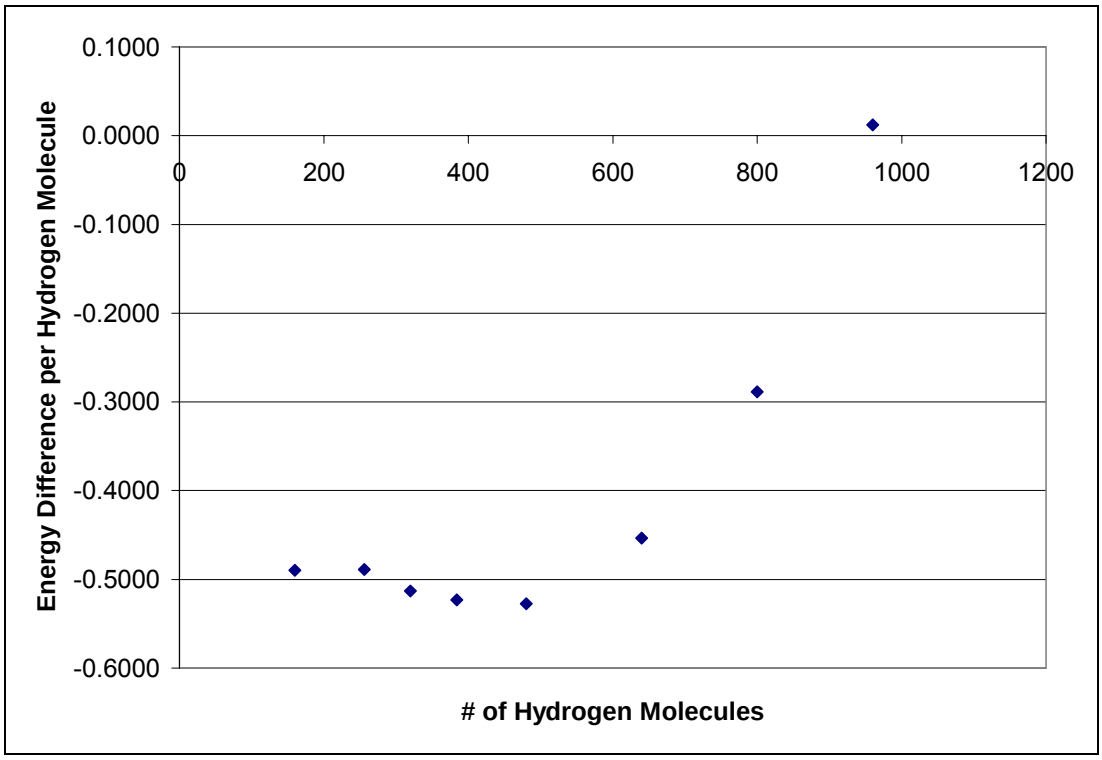

Figure 4.16 Energy difference per H_2 in 7,7 CNT

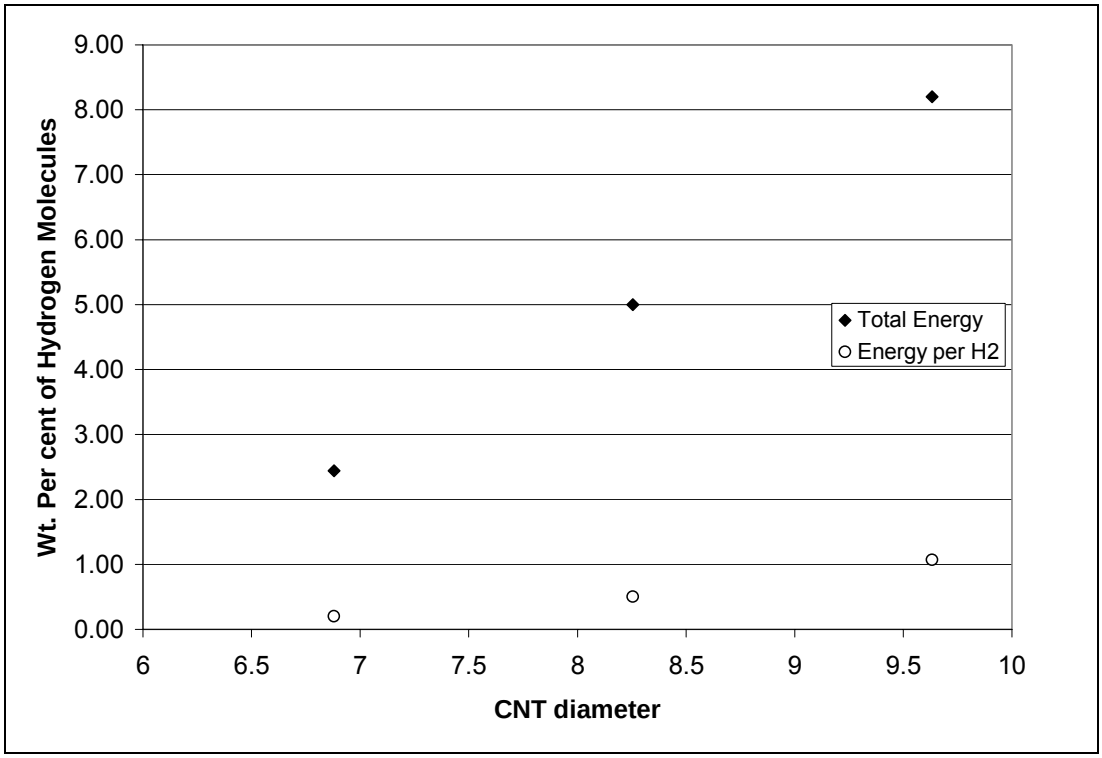

Figure 4.17 Hydrogen storage vs. diameter of CNTs

This result is parallel with the Lee *et al.*'s findings for 5,5 and 10,10 carbon nanotubes [3]. Their work shows that the maximum hydrogen storage capacity increases linearly with diameter of single wall nanotube. Diameter of (10,10) nanotubes is two times of (5,5) nanotube and their results show that (10,10) nanotube can store hydrogen by the load of 2.0, which is two times of the hydrogen coverage of 1.0 for (5,5) nanotubes.

5. CONCLUSIONS

- Carbon nanotube bundles consisting of four nanotubes in a supercell is a very suitable system to study of hydrogen storage capabilities of carbon nanotubes (inside of nanotubes and/or interstitial space between nanotubes) and for comparing the hydrogen storage capacities of different sized nanotubes.

- In this work, empty space inside nanotubes was found more favorable hydrogen storage media compared to the interstitial space between nanotubes. Since the space is larger inside the nanotubes compared to the interstitial space between nanotubes, van der Waal forces between molecules are smaller and, as a result, the total energy of the system is smaller.

- The simulation results showed that carbon nanotubes with larger diameter size have higher hydrogen storage capacity, most probably due to their larger empty space inside; they offer more space for hydrogen storage without being severely effected from van der Waals forces.

- If hydrogen density was assumed to be nearly constant inside the tube, the volume and the number of the hydrogen atoms increases with a square of the radius, whereas the number of carbon atoms increases linearly with the radius. The current study showed that linear relation.

6. RECOMMENDATIONS

- Further study can be made on armchiar carbon nanotubes with larger diameters and also on zig-zag and chiral nanotubes as well to draw a better energy profiles for hydrogen storage capacities.

- This minimization work of hydrogen molecules inside nanotube bundles should be completed by running molecular dynamics simulations on minimized structures.

- The results of this study should be validated with experiments to achieve confidence in the results of molecular dynamics method.

REFERENCES

1. Park, C., P. E. Anderson, A. Chambers, C. D. Tan, R. Hidalgo, and N. M. Rodriguez, "Further Studies of the Interaction of Hydrogen with Graphite Nanofibers", *J. Phys. Chem. B*, Vol. 103, pp. 10572-10581, 1999.

2. Shaijumon, M. M. and S. Ramaprabhu, "Synthesis of Carbon Nanotubes by Pyrolysis of Acetylene Using Alloy Hydride Materials as Catalysts and Their Hydrogen Adsorption Studies", *Chemical Physics Letters*, Vol. 374, pp. 513–520, 2003.

3. Lee, S. M., K. S. Park, Y. C. Choi, Y. S. Park, J. M. Bok, D. J. Bae, K. S. Nahm, Y. G. Choi, S. C. Yu, N. Kim, T. Frauenheim and Y. H. Lee, "Hydrogen Adsorption and Storage in Carbon Nanotubes", *Synthetic Metals*, Vol. 113, pp. 209–216, 2000.

4. Helena, D. and G. Dolgonos, "Molecular Modeling Study of Hydrogen Storage in Carbon Nanotubes", *Chemical Physics Letters*, Vol. 356, pp. 79–83, 2002.

5. Midilli, A., M. Ay, I. Dincer and M. A. Rosen, "On Hydrogen and Hydrogen Energy Strategies I: Current Status and Needs", *Renewable and Sustainable Energy Reviews*, Vol. 9, pp. 255–271, 2005.

6. Ultanir, M. O., *Hidrojenin yakit olarak kullanimi ve ozellikleri*, pp. 295-315, TMMOB Makine Muhendisleri Odasi., 1997.

7. Rosen, M. A. and D. S. Scott, "Comparative Efficiency Assessments for a Range of Hydrogen Production Processes", *Int. Journal of Hydrogen Energy*, Vol. 23(8), pp. 653–659, 1998.

8. Olgun, H., A. Midilli, P. Rzayev and T. Ayhan, *Pyrolysis Studies of Nutshells. Proceedings of 10th International*, Conference on Thermal Engineering and Thermogrammetry (THERMO), Budapest, Hungary, pp.16-21, p. 16–21, 1997.

9. Rand, D. A. J. and R.M. Dell, “The Hydrogen Economy: a Threat or an Opportunity for Lead–acid batteries?”, *Journal of Power Source*, Vol. 144, pp. 568–578, 2005.

10. *Fuel Cell Handbook 6th Edition*, U.S. Department of Energy, 2002.

11. David, E., “An Overview of Advanced Materials for Hydrogen Storage”, *Journal of Materials Processing Technology*, Vol. 162–163, pp. 169–177, 2005.

12. Stan, G. and W. M. Cole, *Journal of Low Temp. Physics*, Vol. 110, pp. 539–544, 1999.

13. Carter, T. and L. Cornish, *Eng. Failure Analysis*, Vol. 8, pp. 113–121, 2001.

14. David, E., V. Stanciu, A. Armeanu, A. Lazar and C. Sandru, *Acta Technica Napocensis,* Vol. 45, pp. 197–202, 2002.

15. Simonyan, V. V. and J. K. Johnson, “Hydrogen Storage in Carbon Nanotubes and Graphitic Nanofibers”, *Journal of Alloys and Compounds*, Vol. 330–332, pp. 659–665, 2002.

16. Chambers, A., C. Park, R. T. K. Baker and N. M. Rodriges, “Hydrogen Storage in Graphite Nanofibers”, *Journal of Physical Chemistry* B, Vol. 102, pp. 4253–4256, 1998.

17. Fan, Y.-Y., B. Liao, M. Liu, Y.-L. Wei, M.-Q. Lu and H.-M. Cheng, *Carbon*, Vol. 37, pp. 1649, 1999.

18. Wang, Q. and J. K. Johnson, Journal of Physical Chemistry B, Vol. 103, pp. 277, 1999.

19. Hirsch, A., “Principles of Fullerene Reactivity. *Top Curr. Chem*, Vol. 199, pp. 1–65, 1999.

20. Fischer, J. E., “Storing Energy in Carbon Nanotubes”, *Chem. Innovation*, Vol. 30, pp. 21–27, 1999.

21. Ye, Y., Ahn C. C., Witham C., Fults B., Lui J., Rinzler A. G., Colbert D., Smith K. A. and Smalley A. E., “Hydrogen Adsorption and Cohesive Energy of Single-walled Carbon Nanotubes”, *Applied Physics Letters*, Vol. 74, pp. 2307–2309, 1999.

22. Dillon, A. C., K. M. Jones, T. A. Bekkedahl, C. H. Kiang, D. S. Bethune and M. J. Heben, “Storage of Hydrogen in Single-walled Carbon Nanotubes”, *Nature*, Vol. 386, pp. 377–379, 1997.

23. Iijima, S. *Nature*, Vol. 354, pp. 56–58, 1991.

24. Ma, Y., X. Yueyuan, Z. Mingwen and Y. Minju, “Structures of Hydrogen Molecules in Single-walled Carbon Nanotubes”, *Chemical Physics Letters*, Vol. 357, pp. 97–102, 2002.

25. Züttel, A., P. Sudan, P. Mauron, T. Kiyobayashi, C. Emmenegger and L. Schlapbach, “Hydrogen Storage in Carbon Nanostructures”, *International Journal of Hydrogen Energy*, Vol. 27, pp. 203–212, 2002.

26. Shiraishi, M., T. Takenobu, H. Kataura and M. Ata, “Hydrogen Adsorption and Desorption in Carbon Nanotube Systems and its Mechanisms”, Applied Physics A, Vol. 78, pp. 947–954, 2004.

27. Dillon, A. C., K. M. Jones, T. A. Bekkedahl, C. H. Kiang, D. S. Bethune and M. J. Heben, *Nature*, Vol. 386, pp. 377, 1997.

28. Ye, Y., C. C. Ahn, C. Witham, B. Fultz, J. Liu, A. G. Rinzler, D. Colbert, K. A. Smith and R. E. Smalley, *Applied Physics Letters*, Vol. 74, pp.2307, 1999.

29. Liu, C., Y. Y. Fan, M. Liu, H. T. Cong, H. M. Cheng and M. S. Dresselhaus, *Science*, Vol. 286, pp. 1127, 1999.

30. Guay, P., B. L. Stansfield and A. Rochefort, "On the Control of Carbon Nanostructures for Hydrogen Storage Applications, *Carbon*, Vol. 42, pp. 2187–2193, 2004.

31. Available at http://www.cmmp.ucl.ac.uk/~Econquest/DFT.html, 2005.

32. Available at http://csep1.phy.ornl.gov/mc/node1.html, 2005.

33. Ma, Y., Y. Xia, M. Zhao, R. Wang and L. Mei, "Effective Hydrogen Storage in Single-wall Carbon Nanotubes", *Physical Review B*, Vol. 63, pp. 115422, 2001.